Science of Remote Sensing 13 (2026) 100383

Contents lists available at ScienceDirect

Science of Remote Sensing

journal homepage: www.sciencedirect.com/journal/science-of-remote-sensing

Satellite remote sensing for estimating reservoir physical characteristics: A global review of existing methodologies for operational monitoring

Audrey Kantz Dossou Codjia [a,b,c,*], Komlavi Akpoti [a], Moctar Dembélé [a], Roland Yonaba [b], Tazen Fowe [b], Triumph Prosper Orowale [c], Modeste G. Déo-Gratias Koissi [a,b], Soumahila Sankande [b], Sander J. Zwart [a]

[a] International Water Management Institute (IWMI), PMB CT 112, Cantonments, Accra, Ghana
[b] International Institute for Water and Environmental Engineering (2iE), P.O. Box 594, Ouagadougou, Burkina Faso
[c] West African Science Service Centre on Climate Change and Adapted Land Use (WASCAL), P.O. Box 9507, Ouagadougou, Burkina Faso

ARTICLE INFO

Keywords:
Reservoir
Satellite remote sensing
Surface area
Volume
Water level

ABSTRACT

Accurate and timely estimates of reservoir surface area, water level, and volume are essential for water resource management. Yet no recent synthesis compares the remote sensing methods used to obtain these physical characteristics. This study evaluates peer-reviewed studies from 2000 to 2025 that derived any of the three characteristics from satellite data to identify reliable techniques and operational gaps. A total of 169 cases of surface area mapping (88), water level retrieval (49), and volume estimation (32) were analyzed from 106 articles across more than 60 countries. Each case was classified according to its physical characteristics, approach, sensor, and validation method. Surface area is typically mapped using optical imagery (76 %). Threshold indices dominate at 63 %. Meanwhile, machine and deep learning methods are being used more frequently to provide more accurate classifications. Water levels are usually obtained from radar altimetry (67 %) followed by area-elevation models (30 %). Volume is most often computed using combined area-elevation approaches (60 %), followed by water level-volume regressions (25 %) and area-volume curves (15 %), with average errors of up to 10 %. Three critical gaps emerge: only 11 % of studies address reservoirs smaller than 1 km^2, turbid or vegetated waters incur estimation errors, and only a few studies use sensors with a revisit time of three days or less, which limits real-time management. Although fusion of several sensor data is demonstrably more accurate, it remains rare. These insights guide managers and future research directions to enable automated, high-resolution monitoring of both large and small reservoirs.

1. Introduction

Water is a fundamental resource for sustaining ecosystems, food security, and supporting human livelihoods. Yet, its spatial and temporal distribution remains highly uneven across the globe, often posing significant challenges for resource planning and management (Sheffield et al., 2018; Famiglietti, 2014). Reservoirs play a crucial role in addressing these challenges by enabling the storage, regulation, and distribution of freshwater for diverse uses including domestic supply, agriculture, hydropower, fisheries, and industrial processes (Crétaux et al., 2015; Wada et al., 2017). They are essential components of the global water system and serve as critical buffers between natural hydrological variability and human demand. Studies have further emphasized their systemic importance in stabilizing regional water availability, contributing to groundwater recharge, mitigating floods, and adapting to climate change by moderating seasonal variability and extreme weather events (Şen, 2021; Li et al., 2023; Donchyts et al., 2022).

However, the sustainable operation and management of reservoirs heavily depend on the timely and accurate collection of information about the quantity and quality of water in reservoirs. Quantifying water in reservoirs is very important and is based on the estimation of physical characteristics, such as surface area, water level, and storage volume (Rodríguez-Alarcón and Lozano, 2017). Traditionally, these parameters have been obtained through in situ measurements using field-based instruments, including limnimeters and bathymetric surveys. While reliable, these methods are often constrained by logistical, financial, and environmental factors – particularly in remote or conflict-affected

* Corresponding author. International Water Management Institute (IWMI), PMB CT 112, Cantonments, Accra, Ghana.
E-mail addresses: kantzcodjia@gmail.com, codjia.k@wascal.org (A.K.D. Codjia).

https://doi.org/10.1016/j.srs.2026.100383
Received 23 June 2025; Received in revised form 5 November 2025; Accepted 28 January 2026
Available online 29 January 2026

regions where regular field monitoring is either cost-prohibitive or physically infeasible (Sagawa et al., 2019; Akpoti et al., 2022). Even in more accessible regions, field data collection efforts may lack the temporal resolution required for dynamic reservoir management or long-term trend analysis (Eldardiry and Hossain, 2021).

In recent decades, Earth Observation (EO) technologies have emerged as effective tools for enhancing all facets of reservoir management at local to global scales (Gao, 2015). Multi-spectral and hyperspectral data are now used to track algal blooms, turbidity, and suspended sediment (Kislik et al., 2022; Hossain et al., 2021). Radar imagery supports monitoring of dam wall deformation and seepage (Pang et al., 2023). Thermal sensors reveal surface temperature stratification and evaporation losses (Li et al., 2024). The analysis of high-temporal-resolution satellite data underpins flood routing, infrastructure safety inspections, and ecological impact assessments (Wang et al., 2023a). This broad range of applications is narrowed down in this review to focus specifically on EO methods for quantifying reservoir water, including surface area, water level, and storage volume. These physical characteristics are essential for both operational decision-making and long-term water security planning.

Optical sensors (e.g., MODIS, Landsat, Sentinel-2) and radar altimetry missions (e.g., TOPEX/Poseidon, Jason series, Sentinel-6) have been successfully applied to map surface water extents, estimate water levels, and compute volumetric changes in both large and small water bodies (Garnier et al., 2024; Codjia et al., 2025; Chen et al., 2024; Kong et al., 2025; Pipitone et al., 2018; Niño et al., 2022; Quang et al., 2021; Hou et al., 2024). Numerous methodologies have been proposed for extracting reservoir characteristics from satellite data, ranging from water indexes and empirical models based on statistical relationships, to more recent developments using artificial intelligence, semi-empirical models, and physics-based hydrodynamic simulations (Casal et al., 2020; Sorkhabi et al., 2022; Hossen et al., 2022). The performance and applicability of these methods vary greatly from one case study to another. EO-based reservoir monitoring methodologies may face several limitations. These include the interplay between sensor characteristics (e.g., resolution and acquisition frequency), data availability, and atmospheric and optical conditions. The geomorphological complexity of the reservoir environment and water quality can also pose a challenge. (Gao et al., 2012a; Psomiadis et al., 2021).

A clear challenge exists in the field of reservoir monitoring. Studies are scattered across sensors, algorithms, and scales, which makes it difficult for managers and even scientists to determine the most effective satellite and appropriate method for reservoir monitoring. Since operational reservoir monitoring involves decisions regarding water allocation, drought response, and dam operation, the usefulness of EO data sources and methodologies depends on their ability to reliably deliver near-real-time, spatially consistent information to management systems. This review therefore:

(i) inventories and classifies the full range of EO data sources and methodologies used to map reservoir surface area, water level/depth, and storage volume;
(ii) compares their accuracy, strengths, and limitations; and
(iii) identifies the practical and research gaps that hinder routine, operational deployment.

The review translates evidence into practical guidance for reservoir managers, water resource agencies, and EO scientists. By linking the proven accuracy, latency, and data demands of each method to specific reservoir contexts, the review pinpoints situations in which a low-cost approach is sufficient, situations in which a more complex method is worth the investment, and areas in which future research should focus. The outcome is a set of clear, prioritized recommendations that can inform day-to-day reservoir management and strategic planning, especially in regions without in-situ networks.

2. Concepts and methodology

2.1. Concepts of satellite remote sensing and reservoir monitoring

Satellite Remote Sensing (RS) has transformed Earth observation by enabling the collection of large-scale and frequent data with increasing spatial and temporal resolution. For example, the Sentinel-2 satellite provides imagery with a spatial resolution of 10–20 m and a revisit time of 3–5 days, while MODIS offers coarser resolution (250–500 m) but with daily coverage (Goetz et al., 1983; Gan et al., 2025).

Satellites function as sensors that detect energy emitted or reflected by objects on the Earth's surface. Based on how they collect this energy, RS systems are typically classified as passive or active. Passive remote sensing systems (e.g., radiometers, spectrometers) rely on detecting solar radiation reflected by surfaces. In contrast, active systems (e.g., radar, LiDAR) emit their own energy and measure the returned signal after interacting with a target (Zhu et al., 2017).

The applications of satellite RS are vast and include agriculture, pasture and forest monitoring, climate and weather studies, urban planning, oceanography, water resources management (WRM), health, archaeology, and telecommunications (Chi et al., 2016; Ashraf et al., 2023). More recently, satellite RS has proven particularly valuable for reservoir monitoring.

Although reservoir monitoring generally involves regular assessments of both water quality and quantity, quantitative (physical) characteristics ultimately determine reservoir dynamics. Conventionally, water quantity through water levels is measured using limnimeters, and bathymetric data are collected using field-based equipment (Ma et al., 2024; Ceylan et al., 2011). These measurements are essential for tracking sedimentation, erosion, and ecosystem changes, as well as for estimating flood control capacity through surface area analysis.

Importantly, combining surface area with water level data enables the estimation of reservoir volume, a critical parameter for water resource management. Accurate volume estimates support water supply planning, hydroelectric power generation (Abd Ellah and El-Geziry, 2016), and equitable water allocation by extension agents and farmers' organizations. The relationships between surface area, height, and volume are commonly visualized through Area-Height, Area--Volume, and Height-Volume curves, which are essential tools for reservoir management (Girard et al., 2025).

Satellite remote sensing enables the estimation of all these physical characteristics - surface area, water level, and volume - through both passive and active sensing technologies. Fig. 1 has been designed to provide an overview of RS-based approaches for reservoir monitoring.

2.2. Assessment of estimation performance

Assessing the accuracy of a method is essential to determine how well it estimates physical characteristics and to identify potential errors introduced during the process. This typically involves comparing the results obtained using the method with reference values derived from reliable sources such as field measurements (Pereira et al., 2019), satellite observations (Pipitone et al., 2018), published literature (Birkett, 2000), or high-resolution imagery from UAVs, aircraft, or commercial satellites (Feyisa et al., 2014). However, in some cases, accuracy assessments are not conducted due to the unavailability of field data.

Accuracy evaluation can be done using various metrics, which are generally grouped into two main categories. The first category includes non-site-specific metrics that compare the estimated values (e.g., surface area, water level, or volume) directly with corresponding reference data, without considering spatial location. These metrics are applicable across all three physical parameters.

Several of these metrics are often used interchangeably under different names. Table 1 presents the formulas and details of some common non-site-specific accuracy assessment parameters.

Despite their usefulness, non-site-specific accuracy assessments have

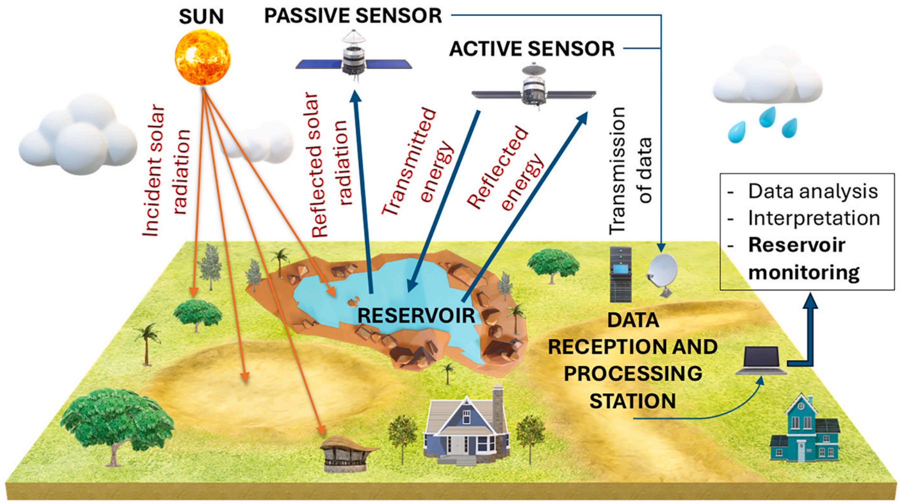

Fig. 1. Overview of reservoir monitoring approaches based on RS.

Table 1
Formulas of some non-site-specific analysis metrics.

Parameter	Acronym	Formula	References
Root Mean Square Error	RMSE	$\sqrt{\frac{1}{n}\sum_{i=1}^{n}(y_i-y'_i)^2}$	Munyaneza et al. (2009)
Normalized Root Mean Square Error	NRMSE	$\frac{\sqrt{\frac{1}{n}\sum_{i=1}^{n}(y_i-y'_i)^2}}{y'_i}\times 100$	Gao et al. (2012a)
Correlation coefficient	r	$\frac{\sum_{i=1}^{n}(y_i-\underline{y})(y'_i-\underline{y}')}{\sqrt{\sum_{i=1}^{n}(y_i-\underline{y})^2}\sqrt{\sum_{i=1}^{n}(y'_i-\underline{y}')^2}}$	Zhu et al. (2014)
Coefficient of determination	R^2	$\frac{Cov(y_i,y'_i)}{D(y_i)D(y'_i)}$	Zhang et al. (2014a)
Bias	Bias	$\underline{y}-\underline{y}'$	Zhang et al. (2014a)
Mean Absolute Error	MAE	$\frac{1}{n}\sum_{i=1}^{n}\lvert y_i-y'_i\rvert$	Zhu et al. (2014)
Mean Square Error	MSE	$\frac{1}{n}\sum_{i=1}^{n}(y_i-y'_i)^2$	Liu et al. (2021)
Percent error	PE	$100\times\frac{y_i-y'_i}{y'_i}$	Pereira et al. (2019)
Mean Absolute Percentage Error	MAPE	$\frac{1}{n}\sum_{i=1}^{n}\lvert PE_i\rvert$	Pereira et al. (2019)
Nash–Sutcliffe coefficient	NSE	$1-\frac{\sum_{i=1}^{n}(y'_i-y_i)^2}{\sum_{i=1}^{n}(y'_i-\underline{y}')^2}$	Kale and Acarlı (2019)
Standard Deviation	STD	$\sqrt{\frac{1}{n-1}\sum_{i=1}^{n}\left[(y_i-y'_i)-(\underline{y}-\underline{y}')\right]^2}$	Cheng et al. (2022)
Normalized Difference Area Index	NDAI	$\frac{y'_i-y_i}{y'_i+y_i}$	Annor et al. (2009)
Deviation Area Index	DAI	$\frac{y'_i-y_i}{y'_i}$	Annor et al. (2009)

y' is the value of the physical characteristic such as surface area, water level, and water volume of reference data, y is the estimated corresponding variable, $\underline{y}$ and $\underline{y}'$ are the mean value of y and y', respectively, i is the index of the variable, and n is the number of the sample size. Cov() means covariance and D() represents the variance.

certain limitations. As highlighted by Congalton et al. (2001) (Congalton, 2001), these metrics do not account for the spatial correctness of classified pixels. For instance, in surface area estimation, such metrics only compare aggregated values of physical characteristics with reference data, without assessing the accuracy of the pixel-level classification itself. To address this, additional evaluation metrics tailored to image classification are employed.

Image classification accuracy is commonly assessed using a confusion matrix (also called an error matrix or contingency table), which compares the predicted classes with actual reference classes. Based on this matrix, several key metrics are used in the literature, including the ones presented in Table 2.

2.3. Data and search methodology

The information used in this review was gathered through comprehensive searches on academic search engines, primarily Google Scholar and Scopus. These platforms facilitated access to a wide range of scholarly sources, including peer-reviewed journal articles, books, conference proceedings, theses, dissertations, preprints, abstracts, technical reports, and other relevant scientific literature.

To refine the search process, a nested search strategy was employed. This method involves the use of Boolean operators (AND, OR) and parentheses to combine multiple search terms effectively (Noruzi, 2005; Akpoti et al., 2019). The use of an asterisk (*) enabled the inclusion of term variants and alternative spellings. Fig. 2 illustrates a visual example

Table 2
Some accuracy assessment metrics based on confusion matrix.

Metric	Abbreviation	Formula/Notes	Reference
Probability of Detection	POD	POD = TP/(TP + FN)	Khan et al. (2011)
False-Alarm Ratio	FAR	FAR = FP/(TP + FP)	Khan et al. (2011)
Critical Success Index	CSI	CSI = TP/(TP + FP + FN)	Khan et al. (2011)
Accuracy	ACC	ACC = (TP + TN)/(TP + FP + TN + FN)	Liu et al. (2021)
Precision	–	Precision = TP/(TP + FP)	Liu et al. (2021)
Recall (Sensitivity)	–	Recall = TP/(TP + FN)	Liu et al. (2021)
Fβ-Score (β = 1)	F1-Score	F1 = 2 × (Precision × Recall)/(Precision + Recall)	Liu et al. (2021)
Fβ-Score (β = 2)	F2-Score	$F2 = (1 + \beta^2) \times$ (Precision × Recall)/(β^2 × Precision + Recall); here, β = 2	He et al. (2017)
Mean Intersection Over Union	mIoU	mIoU = Mean of (TP/(TP + FP + FN)) across all classes	Liu et al. (2021)
Overall Accuracy	OA	OA = Total correct classifications/Total number of samples	(Codjia et al., 2025; Ghansah et al., 2022)
Producer's Accuracy	PA	PA = TP/(TP + FN)	(Codjia et al., 2025; Ghansah et al., 2022)
User's Accuracy	UA	UA = TP/(TP + FP)	(Codjia et al., 2025; Ghansah et al., 2022)
Kappa Coefficient	Kappa	Varies; ranges from −1 (complete disagreement) to 1 (perfect agreement)	(Codjia et al., 2025; Ghansah et al., 2022)
Average Accuracy	AA	AA = Mean of individual class accuracies	Mylona et al. (2018)
Quantity Accuracy	QA	Part of quantity and allocation disagreement analysis	Tian et al. (2017)
False Alarm Rate	FA	FA = FP/(FP + TN) or similar variation depending on context	Amitrano et al. (2017)
False Positive Rate	FPR	FPR = FP/(FP + TN)	Fisher et al. (2016)
Completeness	Comp	Comp = TP/(TP + FN)	Duy (2015)
Correctness	Corr	Corr = TP/(TP + FP)	Duy (2015)
Quality	–	Quality = TP/(TP + FP + FN)	Duy (2015)

TP: True Positives, FP: False Positives, TN: True Negatives, FN: False Negatives

of the search process using this strategy.

2.4. Data processing

After the literature searches, English-language filtering and de-duplication were applied first. Of the remaining 1200 unique records, only those focusing on reservoirs or lakes and using satellite remote sensing to estimate physical characteristics such as surface area, water level, or volume were retained. Studies limited to general surface water detection or water quality were excluded (reducing the number of records to 315 for full-text assessment). The full texts were then evaluated based on clearly described inputs and methods, as well as representative sensor-method combinations. Multiple papers that duplicated the same setup without added methodological novelty were avoided, while a small number of methodological papers directly applicable to reservoir or lake extent estimation were retained. The final dataset comprises 106 peer-reviewed articles. The retained documents were assembled to form a database in Mendeley. A set of information has been extracted from the documents and organized in a synoptic table. Table 3 presents the set of information collected.

The extracted information enabled analysis according to the physical characteristics measured by the studies. First, the type of sensor used for each reservoir characteristic is assessed. Then, the approach used is examined, and the methods employed are compared. Finally, the accuracy reported in the studies is analyzed to determine high-performance sensors and approaches. The effects associated with reservoir size are integrated into all sections of the analysis. Finally, recommendations are provided for the most effective approaches to estimating reservoir physical characteristics using remote sensing.

3. Results and discussions

3.1. Summary of the synoptic table

A total of 106 documents met our inclusion criteria. Original research articles remain dominant (94.1 %), followed by conference

Table 3
Information extracted from documents.

Information extracted	Description
General information on the document	Reference (authors, title, year of publication), type of document (original research article, proceedings, reports, …), country or region
Study area	Name of the studied reservoirs, number of reservoirs, size of the reservoir, depth of the reservoir
Studied physical characteristics	Surface areas, water levels/bathymetry, storage/ volumes
Approach used	Type of approach used, specific method used, used algorithms or models, software or tool used
Performance evaluation	Accuracy assessment metrics and their values, type of data used for validation, precise data used for validation, validation metrics and their values
Satellite types and their characteristics	Name of satellite, type of sensor, bands, temporal and spatial resolution, area covered, availability, launch date, end date

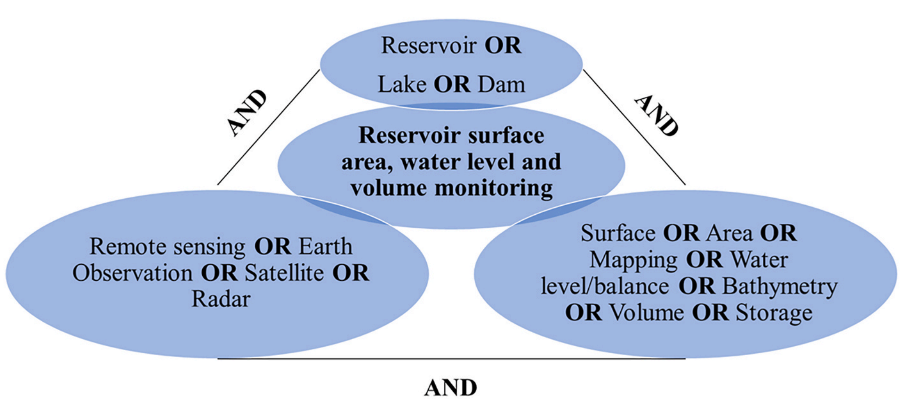

Fig. 2. Nested search terms used.

proceedings (4.7 %) and technical reports (1.2 %). Publication years range from 2000 to 2025, with two peaks in 2019 and 2024 (21 and 22 papers each) (see Fig. 3).

The literature now spans more than sixty different countries and territories. A Of the study areas, Asia accounts for approximately 47 % of them, followed by Africa (17 %), the Americas (13 %), and Europe (12 %). Oceania contributes approximately 2 %, and 8 % of the studies are global or multi-country. Fig. 4 shows the spatial distribution of the study areas.

The studied reservoirs have surface areas of more than 69 000 km^2. Based on the classification of Annor et al. (2009) only 11 % of studies focused on small reservoirs (with a size limit of 1 km^2) (Annor et al., 2009). The other reservoirs being large can be either natural lakes, man-made reservoirs, rivers, or bays. Regarding the depth of these reservoirs, the classification was made according to the sensitivity of the types of sensors used for a certain depth range. The sensible depths for passive sensors can reach 30 m (Ashphaq et al., 2021). Reservoirs less than 30 m deep were therefore considered shallow. In this study, 77.4 % of the reservoirs are deep while 22.6 % are shallow. While some studies deal with only one of the physical characteristics (surface area, water level, or volume), others combine two or three. Papers reporting multiple distinct combinations contributed to multiple cases, yielding 169 method-specific cases in total. Across the enlarged database, surface area retrieval remains the most frequent objective, appearing 88 times, while water level estimation is addressed 49 times and 32 derive storage volumes.

3.2. Passive sensors for reservoir surface area estimation

Due to its unique backscatter and emissivity characteristics, water responds to radiation differently than most other surface materials. These distinctive properties enable various satellites, equipped with passive or active sensors, to reliably detect water bodies on Earth's surface (Gao, 2015).

The spectral resolution of satellites plays a crucial role in detecting water-covered surfaces, as it determines the number and range of wavelengths (bands) the satellite can observe. Satellites that capture imagery in the Short-Wave Infrared (SWIR) range (1100–3000 nm), as well as in the Visible and Near Infrared (VIS-NIR) range (approximately 400–900 nm), are particularly effective at identifying water bodies (Bijeesh and Narasimhamurthy, 2020). Three-quarters (about 76 %) of the documented surface area studies rely on optical satellite sensors.

Satellites such as Landsat, Sentinel-2, and MODIS – which include SWIR bands – are especially suited for delineating water surfaces, as water absorbs strongly in the SWIR range. These satellites are widely used in research to generate accurate water body maps (Arsen et al., 2013; Krivoguz et al., 2020; Wu and Liu, 2015).

Even satellites that lack SWIR bands but capture data in the VIS-NIR range can still be used for water detection. However, these sensors often struggle to distinguish water from other materials like dry or wet soil, especially in cases where the water is turbid, contains suspended sediments, or is covered with aquatic vegetation (García et al., 2016). For example, AVHRR and FORMOSAT-2, which lack SWIR capabilities, have nonetheless been successfully used to monitor the surface extent of Lake Chad and Lake La Bure, respectively (Birkett, 2000; Baup et al., 2014).

The choice of satellite imagery for water body monitoring also depends on the spatial and temporal resolution of the sensors. Spatial resolution refers to the ground area represented by a single pixel in the image – the finer the spatial resolution, the more detailed the water body can be mapped. Huang et al. (2018) (Huang et al., 2018) classified optical sensors into three categories based on spatial resolution:

– Coarse Spatial Resolution Sensors: >200 m
– Medium Spatial Resolution Sensors: 5–200 m
– High Spatial Resolution Sensors: <5 m

Temporal resolution, or revisit time, indicates how often a satellite passes over the same location. Higher temporal resolution is critical for monitoring dynamic water bodies. A summary of commonly used optical sensors for water extent mapping is provided in Table 4.

Table 4 shows that authors rely heavily on free, medium-resolution satellites, especially Landsat (30–80 m, 16-day revisit) and Sentinel-2 (10–60 m, 5-day revisit) utilized in over 30 studies and at least six studies respectively. These satellites offer worldwide coverage, open-access data, and adequate detail for reservoir mapping. Landsat imagery particularly allows long-term analysis. The use of the other medium resolution satellites is diverse; they were used only once or twice. Their limited usage is due to commercial pricing (SPOT-5) or restricted regional data availability (HJ-1A/B). The adoption of SDGSAT-1 (MII) for reservoir mapping is only beginning to appear in the literature because it is a relatively new mission, launched in 2021 (Jiang et al., 2024).

Four sensors appear for the coarse resolution sensors. They account for nine studies, with MODIS (250–1000 m, 0.5 day revisit) used in up to four studies. While they have a good temporal resolution, the spatial coarse resolution of these sensors limits their ability of mapping small or narrow reservoirs.

High-resolution satellites (less than 10 m) such as Pléiades, FORMOSAT-2, Flock 2 satellites, WorldView-2, and Gaofen-1 (GF1) provide the finest detail (He et al., 2017; Baup et al., 2014; Ma et al.,

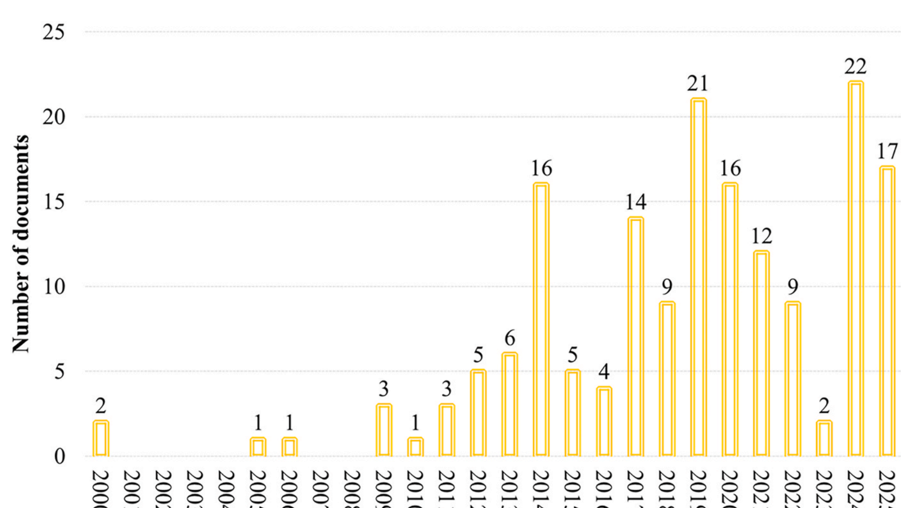

Fig. 3. Number of documents per year reviewed per year between 2000 and 2025.

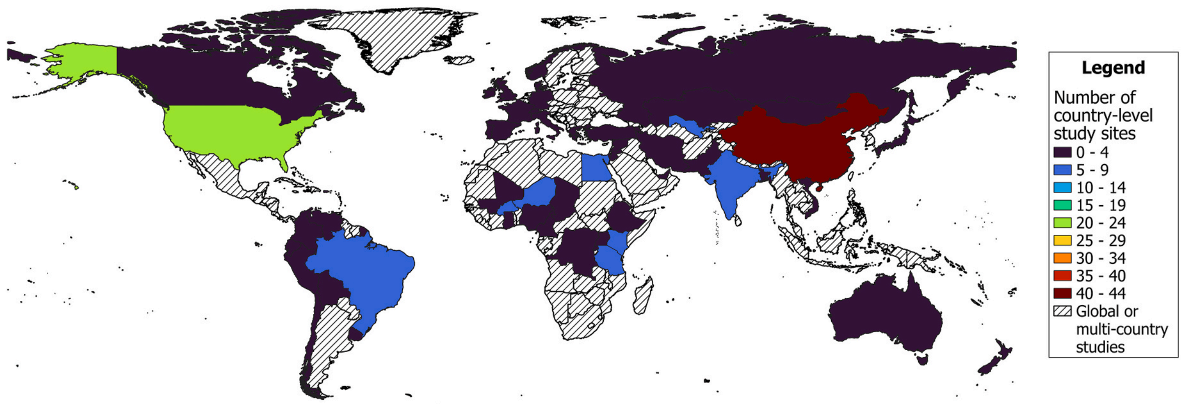

Fig. 4. Spatial distribution of study areas.

Table 4
Optical sensors used for surface water detection.

Sensor group	Satellite	Number of bands	Temporal resolution	Spatial resolution	Coverage area	Availability	Launch date	End date	Documented usage in literature
Coarse spatial resolution	Meteosat 2-7	12	30 min	5 Km	Limited	Free	1986	2001	1 study
	AVHRR	5	1 day	1100 m	Global	Free	1981	–	2 studies
	Sentinel 3 (SLSTR)	9	27 days	500 m to 1 Km	Global	Free	2016	–	2 studies
	MODIS	36	0.5 days	250–1000 m	Global	Free	1999	–	4 studies
Medium spatial resolution	HJ-1A/B	4 to 115	4 days	30 m–300 m	Limited	Free	2008	–	1 study
	Landsat 1-9	4 to 9	16 days	30–80 m	Global	Free	1972	–	30+ studies
	SPOT-5	5	26 days	2.5–20 m	Limited	Commercial	1986	–	1 study
	ASTER	14	16 days	15 m–90 m	Global	Free	1999	–	2 studies
	Sentinel 2	13	5 days	10–60 m	Global	Free	2015	–	6+ studies
	SDGSAT-1 (MII)	7	11 days	10 m	Global	Free	2021	–	1 study
High spatial resolution	FORMOSAT-2	5	1 day	2–8 m	Limited	Commercial	2004	–	1 study
	Flock 2 satellites	4	1 day	3–5 m	Limited	Commercial	2015	–	1 study
	Pléiades	5	26 days	0.5 m	Limited	Commercial	2012	–	1 study
	WorldView-2	9	1.1 days	0.46 m–1.85 m	Limited	Commercial	2009	–	1 study
	Gaofen-1 (GF1)	5	4 days	1–16 m	Limited	Commercial	2013	–	1 study

2020; Minghelli et al., 2020). However, they are used in only five studies since their imagery is commercial and limited to some regions.

The number of spectral bands does not necessarily affect the choice of satellite by the authors. Despite their frequent gaps related to cloud cover, optical sensors are the preferred for waterbody mapping.

3.3. Active sensors for reservoir surface area estimation

Active sensors offer significant advantages over passive sensors in addressing challenges associated with water extent mapping, particularly under cloudy, rainy, or low-light conditions. Unlike passive sensors, active sensors emit their own radiation, enabling them to penetrate the atmosphere and clouds, and operate effectively regardless of daylight or weather conditions. Among these, Synthetic Aperture Radar (SAR) systems are especially prominent. SAR transmits microwave signals – either horizontally (H) or vertically (V) polarized – toward the Earth's surface and records the backscattered energy to generate high-resolution images (Brisco, 2015). This capability allows SAR to detect scattering mechanisms and distinguish between surface features, making it highly effective for mapping inundated areas, even at night or during adverse weather events. Shorter wavelengths correspond to higher frequencies, and this relationship plays a key role in determining the performance of active sensors for water detection. Table 5 presents some active sensors used for surface area determination.

Table 5 shows that most authors use C-band radar satellites and especially Sentinel-1, which appear in 5 of the 16 studies listed. According to Ottinger and Kuenzer (2020), C-band instruments are among the most widely used in water resource management applications due to their favorable balance between penetration ability and spatial resolution (Ottinger and Kuenzer, 2020). These sensors send longer waves (about 5 cm) that pass through clouds, have 5–50 m of resolution, and a revisit time of 12–35 days, which is good for regular reservoir monitoring. Prominent satellites equipped with C-band SAR include Envisat-ASAR, RADARSAT-2, and Sentinel-1, which have been extensively used for surface water monitoring. Vickers, Malnes, and Høgda (2019), developed a methodology to map lake surface water cover using 13 years of SAR data from Sentinel-1, RADARSAT-2, and Envisat-ASAR (Vickers et al., 2019).

Satellites with X-bands such as TerraSAR-X (TanDEM-X) and Cosmo SkyMed provide higher resolution imagery (down to 1 m) and a revisit time of 3–16 days. For instance, Amitrano et al. (2017) used Cosmo SkyMed in a semi-arid region of Burkina Faso to effectively map small reservoirs (Amitrano et al., 2017). The main issue with such satellites is that their data is sold commercially, which is why they are only used in five studies.

SRTM mission flew only once in 2000 but produced a free, global elevation map at 30 m that a few authors used to delineate permanent water.

Despite their proven utility, the operational application of active sensors can be constrained by limitations in spatial and temporal resolution compared to optical sensors, which may affect the precision and timeliness of water management decisions (García et al., 2016).

Table 5
List of some active sensors used for surface area determination.

Satellite	Bands	Frequency	Temporal resolution	Spatial resolution	Coverage area	Availability	Launch date	End date	Documented usage in literature
Sentinel 1	C-Band (3.8–7.5 cm)	5.405 GHz	12 days	5 m * 5 m–5 m * 20 m	Global	Commercial	2014	–	5 studies
TerraSAR-X (TanDEM-X)	X-Band (2.4–3.8 cm)	9.65 GHz	3 days	1.1–18.5 m	Global	Commercial	2007	2010	3 studies
ENVISAT - ASAR	C-Band (3.8–7.5 cm)	5.3 GHz	35 days	30 m	Global	Commercial	2002	2012	3 studies
Cosmo SkyMed	X-Band (2.4–3.8 cm)	9.6 GHz	16 days	1–100 m	Global	Commercial	2007	–	2 studies
RADARSAT-2	C-Band (3.8–7.5 cm)	5.405 GHz	24 days	3–100 m	Global	Commercial	2002	2012	2 studies
SRTM	C-Band (3.8–7.5 cm) & X-Band (2.4–3.8 cm)	5.3 & 9.6 GHz	NA	30 m–90 m	Global	Free	2000	–	1 study

3.4. Multi-sensor data fusion

Thirteen papers present multi-sensor fusion for surface area mapping, which follows three clear patterns. First, optical and SAR fusion combines Sentinel-1 backscatter with Sentinel-2 and/or Landsat 8/9 reflectance. This fusion can be implemented as either feature-level fusion, which involves stacking SAR and optical features into one classifier input, or decision-level fusion, which involves creating independent water masks per sensor and then combining them (Schmitt, 2020; Li et al., 2022; Tavus et al., 2020; Druce et al., 2021; Declaro and Kanae, 2024). Second, spatiotemporal fusion integrates optical sensor data from multiple sources, such as MODIS and Landsat, achieving Landsat-like spatial detail at a higher temporal frequency. Wang et al. (2023) and Peng et al. (2025) employed the model-based Enhanced Spatial and Temporal Adaptive Reflectance Fusion Method (ESTARFM) in their studies (Peng et al., 2025; Wang et al., 2023b). Other researchers, including Wu et al. (2023), Zheng and Lv (2025), and Filali et al. (2024), use learning-based optical fusion (Filali et al., 2024; Wu et al., 2023; Zheng and Lv, 2025). Rao et al. (2019) fused two MODIS products (MOD09A1 and MOD13Q1) to densify lake extent series using HDSTAFM (Homologous Data-Based Spatial and Temporal Adaptive Fusion Method) (Rao et al., 2019). Conversely, Miura et al. (2025) created harmonized Landsat 8 and Sentinel-2 water-index composites (with no pixel or feature fusion) for monthly mapping (Miura et al., 2025). Third, cross-modal image synthesis is used to bridge sensing gaps. Carbonneau (2025) used style transfer from Sentinel-1 to Sentinel-2 (with long-term Sentinel-2 mosaics) to generate synthetic, optical-like inputs that enable water delineation when optical scenes are unavailable (Carbonneau, 2025). These studies demonstrate consistent sensor pairings and a coherent set of fusion categories (pixel, feature, and decision levels; model-based learning). Each category is chosen to exploit complementary revisit, cloud tolerance, and spectral information to map the extent of surface water.

3.5. Approaches used for reservoir surface area estimation

Depending on the type of sensor and the specific objectives of a study, various approaches are employed to extract reservoir surface areas from satellite imagery. While the fundamental principles for processing data from both passive and active sensors are generally similar, working with active sensors – particularly SAR – often involves more complex procedures. This complexity arises from several sources of error that can affect SAR data, including water-like surface backscatter, speckle noise, and geometric distortions (Shen et al., 2019). Therefore, thorough pre-processing steps such as geo-referencing, ortho-rectification, and speckle filtering are essential for ensuring data accuracy (Grimaldi et al., 2016). Similarly, multi-sensor data fusion uses the same basic methods for mapping reservoirs.

A wide range of methodologies have been applied to map water extents. In some cases, researchers use readily available data products and tools, such as the Global Surface Water Explorer (GSWE) (Pereira et al., 2019). Developed by the European Commission's Joint Research Centre in collaboration with UN Environment and Google, the GSWE serves as a "virtual time machine" by providing global water maps over a period of more than three decades. This platform enables users to extract key indicators such as maximum water extent (Li et al., 2021).

In the following section, the most common approaches used for reservoir surface mapping based on their underlying principles are grouped. Four main methodological categories will be presented and discussed.

3.5.1. Threshold-based approaches

Threshold-based approaches use either a single band from satellite imagery or a water-specific spectral index to delineate water bodies, and they account for 63 % of the reviewed studies. In the case of optical sensors, wavelengths in the Shortwave Infrared (SWIR; 1250–2500 nm), Near-Infrared (NIR; 700–1250 nm), or Visible (VIS; 350–700 nm) ranges are commonly exploited, as water absorbs energy differently across these bands (Gao, 2015). Single-band or multi-band thresholding techniques have been widely employed in the past for water extent mapping (Garnier et al., 2024). For example, Sethre et al. (2005) used Landsat TM Band 5 to detect prairie pothole ponds in the Devils Lake Basin, North Dakota (Sethre et al., 2005). Similarly, this method was applied to Landsat imagery to estimate the surface area of Lake Poopó in Bolivia, covering approximately 2500 km^2 (Arsen et al., 2013).

Pixel histogram-based methods focus on the distribution of pixel values. When a bimodal histogram (representing water and non-water pixels) is observed, automatic thresholding methods such as the Otsu algorithm can be used (Cheng et al., 2022; Vanthof and Kelly, 2019; Zhang et al., 2020). For non-bimodal histograms, defining Regions of Interest (ROIs) through visual interpretation becomes necessary – a process that is subject to human error. Manual delineation using software such as ERDAS Imagine, ENVI, or ArcGIS has also been reported (Kale and Acarlı, 2019; Ghebreyesus et al., 2016). To address both unimodal and bimodal histograms, Shen et al. (2019) introduced an approach based on the Valley-Emphasis method and its modified version (Shen et al., 2019). Duy (2015) successfully applied these methods using Sentinel-1 imagery to map Thac Ba Lake in Vietnam (Duy, 2015). Another notable pixel histogram-based method is the Local Isoluminance Contour (LIC) algorithm, which Birkett (2000) used for calculating the surface area of Lake Chad (Birkett, 2000).

Image segmentation techniques, which combine morphological and radiometric information, offer enhanced efficiency compared to simple thresholding methods. Among these, the Region Growing Algorithm (RGA) has been employed to generate spatially homogeneous water maps (Cao et al., 2019). Similarly, the Active Contour Method (ACM) has been used for surface water detection in high-resolution TerraSAR-X imagery (Hahmann and Wessel, 2010).

Spectral water index-based methods are among the most widely used approaches for water extent mapping. These methods rely on simple arithmetic operations – such as addition, subtraction, or division – to differentiate water surfaces from other land covers. Although easy and effective, they can be influenced by factors such as atmospheric particles (in optical data) and water quality variations (Gao, 2015). Sometimes, water indices are combined with vegetation indices like the Normalized Difference Vegetation Index (NDVI) to improve accuracy (Lu et al., 2011). Over time, several water indices have been developed, and a summary of those frequently cited in the literature is presented in Table 6. For some indices, only the names of the authors who developed them are mentioned.

- For Landsat 5 Thematic Mapper (TM) and 7 ETM+ (Enhanced Thematic Mapper Plus), the Wavelengths in μm are: ρ_{Blue}: 0.45–0.52; ρ_{Green}: 0.52–0.60; ρ_{Red}:0.63–0.69; ρ_{NIR}: 0.76–0.90; ρ_{SWIR1}: 1.55–1.75; ρ_{SWIR2}: 2.08–2.35.
- For Landsat 5 Multispectral Sensor (MSS) and Landsat 5 TM, the Wavelengths in μm are: ρ_{Green}: 0.50–0.60; ρ_{NIR}: 0.80–1.10; ρ_{SWIR}: 1.55–1.75.
- For MODIS: $C_1 = 6$; $C_2 = 7.5$; G = −2.5; L = 1.
- For Sentinel-1, β_{vh} and β_{vv} represent the backscattering coefficient in VH polarization and VV polarization, respectively.

Several software and application programming interfaces (APIs) are commonly used to calculate water indices, including Google Earth Engine (GEE), ENVI, QGIS, and R. Among these, GEE is the most widely utilized. It is a cloud-based platform that integrates a multi-petabyte catalogue of satellite imagery and geospatial datasets with planetary-scale analysis capabilities, facilitating efficient and large-scale water surface mapping (Yılmaz and Selim, 2024).

Systematic index inter-comparison on Landsat-OLI scenes has shown that no single water index is universally optimal, underscoring the need for adaptive thresholds (Chen et al., 2024). Liu et al., 2024 used a probability function to describe the frequency histogram of NDWI applied to Qinghai Lake (Liu et al., 2024a).

Beyond basic thresholding, other techniques such as Change Detection are also employed for mapping water bodies. Change Detection compares the current state of a water body with a known reference situation. Hostache, Matgen, and Wagner, 2012, explored the process of selecting the most appropriate reference SAR image from online archives (Hostache et al., 2012). Their study demonstrated that, after choosing a reference image from the same period of the year as the image to be analyzed, it is crucial to build a time series of the site and statistically assess variations in water cover based on changes in backscattering behavior. During this process, anomaly indices are calculated to detect significant changes.

Similarly, Amitrano et al. (2017) developed the Seasonal Water Presence Pseudo-Probability (SWPP) approach for detecting seasonal water changes in Yatenga, a semi-arid region of Burkina Faso (Amitrano et al., 2017). This method was applied using Cosmo-SkyMed imagery to effectively monitor surface water dynamics.

3.5.2. Image classification-based approaches

Image classification-based approaches for water surface mapping are part of what is called computer vision and mainly involve machine learning and deep learning techniques - artificial intelligence (AI). These methods include supervised classification, unsupervised classification, ensemble methods for classification, and Convolutional Neural Networks (CNNs). Classification algorithms predict the category to which each data point belongs.

Supervised classification requires training the classifier using labeled data (Baup et al., 2014). Among the simplest supervised classification algorithms is K-Nearest Neighbors (K-NN), a non-parametric learning technique. K-NN was employed for classifying Pleiades satellite images alongside Support Vector Machine (SVM) and Decision Tree algorithms (Nurwauziyah et al., 2018). The Decision Tree algorithm incrementally splits a dataset into smaller subsets while developing an associated decision tree, which can then be used for image classification. This approach was applied for mapping surface water across Cambodia and the Vietnamese Mekong Delta using Sentinel-1 SAR observations (Pham-Duc et al., 2017) and for delineating the surface of Lake Gregory

Table 6
Summary of some water indexes.

Index	Acronym	Formula	Reference
Tasseled Cap Wetness	TCW	$0.1509\rho_{Blue} + 0.1973\rho_{Green} + 0.3279\rho_{Red} + 0.3406\rho_{NIR} - 0.7112\rho_{SWIR1} - 0.4572\rho_{SWIR2}$	Crist (1985)
Normalized Difference Water Index	$NDWI_1$	$\frac{\rho_{Green} - \rho_{NIR}}{\rho_{Green} + \rho_{NIR}}$	McFEETERS (1996)
Modified Normalized Difference Water Index	mNDWI	$\frac{\rho_{Green} - \rho_{SWIR}}{\rho_{Green} + \rho_{SWIR}}$	Xu (2006)
Ouma Water Index	OWI	$f(TCW \pm k, NDWI_2)$, where k = constant; $NDWI_2 = \frac{\rho_{SWIR1} - \rho_{NIR}}{\rho_{SWIR1} + \rho_{NIR}}$	Ouma and Tateishi (2006)
Open Water Classification	OWC	$f\ (SWIR_1, SWIR_2, NDWI_3, NDVI, MrVBF)$, where: $MrVBF = f(Elevation)$ $MrVBF = Multiresolution\ index\ of\ Valley\ Bottom\ Flatness$ $NDWI_3 = \frac{\rho_{NIR} - \rho_{SWIR1}}{\rho_{NIR} + \rho_{SWIR1}}$ $NDVI = \frac{\rho_{NIR} - \rho_{Red}}{\rho_{NIR} + \rho_{Red}}$	Guerschman et al. (2011)
Automated Water Extraction Index	AWEI	$AWEI_{nsh} = 4 \times (\rho_{Green} - \rho_{SWIR}) - (0.25\rho_{NIR} - 2.75\rho_{SWIR2})$ (For locations with no prominent shadow effect) $AWEI_{sh} = (\rho_{Blue} + 2.5\rho_{Green}) - 1.5(\rho_{NIR} + \rho_{SWIR1}) - 0.25\rho_{SWIR2}$ (For locations with prominent shadow effect)	Feyisa et al. (2014)
Automated Method for Extracting Rivers and Lakes	AMERL	$f(NDWI, mNDWI, AWEI_{nsh}, AWEI_{sh})$	Jiang et al. (2014)
Water Index	WI_{2015}	$1.7204 + 171\rho_{Green} + 3\rho_{Red} - 70\rho_{NIR} - 45\rho_{SWIR1} - 71\rho_{SWIR2}$	Fisher et al. (2016)
Combination Water Index	CWI	Combination of mNDWI and EVI (Enhanced Vegetation Index) and NDVI $EVI = G \times \frac{\rho_{NIR} - \rho_{Red}}{\rho_{NIR} + C_1\ \rho_{Red} - C_2\ \rho_{Blue} + L}$ C_1 and C_2 are wavelength-specific aerosol resistance terms; G is a gain factor; L is the canopy background adjustment	Zou et al. (2017)
Sentinel-1 Water Index	SWI	$SWI = 0.1747 \times \beta_{vv} + 0.0082 \times \beta_{vh} \times \beta_{vv} + 0.0023\beta_{vv}^2 - 0.0015 \times \beta_{vh}^2 + 0.1904$	Tian et al. (2017)
Normalized Difference Vegetation Index	NDVI	$NDVI = \frac{\rho_{NIR} - \rho_{Red}}{\rho_{NIR} + \rho_{Red}}$	Mohebzadeh and Fallah (2019)
Normalized Difference Lake Index	NDLI	$NDLI = \frac{\rho_{Red} - \rho_{NIR}}{\rho_{Red} + \rho_{NIR}}$	Chipman (2019)
Enhanced Lake Index	ELI	$ELI = EVI\ (For\ MODIS) = G \times \frac{\rho_{NIR} - \rho_{Red}}{\rho_{NIR} + C_1\ \rho_{Red} - C_2\ \rho_{Blue} + 1}$	Chipman (2019)

in Australia using Landsat imagery (Soltani et al., 2021). The SVM algorithm, based on linear algebra to transform and solve classification problems, has also been widely used for water body extraction. For instance, SVM was applied to map water bodies in Lake Burdur, Turkey (Sarp and Ozcelik, 2017).

Unsupervised classification methods do not require prior training data. Instead, they automatically group pixels based on statistical properties, uncovering hidden structures within the data (Leblanc et al., 2011). Among these methods, K-means clustering is the most frequently used for determining reservoir surface areas (Hossen et al., 2022; Vickers et al., 2019; Gao et al., 2012b; Zhang et al., 2014b; Dardanelli et al., 2014). In simple cases, K is set to 2, separating water from non-water classes. Another method, ISODATA, clusters data based on Euclidean distances between features and has been used by several authors for water mapping (Khan et al., 2011; Song et al., 2013; Singh et al., 2015). Additionally, hierarchical correlation-based clustering was utilized to classify lake surface area time series data in the Yukon Flats ecoregion (Rey et al., 2019). Another unsupervised approach, Online Adaptive Possibilistic C-Means (OAPCM), processes pixels individually to form clusters and was applied to Sentinel-2 images for detecting water extents in the Northern Pindos National Park (Mylona et al., 2018).

Ensemble Methods for Classification combine multiple learning models to improve prediction accuracy. Random Forest (RF), an ensemble algorithm based on bagging, aggregates results from several Decision Trees using binary logic (Codjia et al., 2025). RF was applied within GEE by Ghansah et al. (2022) for mapping small reservoirs and by Psomiadis et al. (2019) for delineating the Bramianos dam in Greece (Psomiadis et al., 2021; Ghansah et al., 2022). Gradient Boosting is another ensemble technique that combines weak learners to reduce bias. Extreme Gradient Boosting (XGBoost), a powerful variant, was employed for water extent mapping in the Amazon Basin (He et al., 2017).

These classification methods are implemented across various platforms, including ENVI, ArcGIS, Google Earth Engine (GEE), VIPER Tools, Keras, Sentinel Application Platform (SNAP), and the Generic Synthetic Aperture Radar (GSAR) suite.

In recent years, deep learning-based methods have emerged as powerful tools for water body mapping. Among them, Convolutional Neural Networks (CNNs) have shown particular promise, classifying each pixel into a specific category (He et al., 2017; Weng et al., 2025; Abid et al., 2021). However, CNNs often involve complex architecture, generate large volumes of parameters, require extended training times, and result in heavy datasets. To address these challenges, Liu et al. (2021) developed the Lightweight Area and Edge Network (LaeNet), a novel CNN architecture combining semantic feature extraction, area segmentation, and edge detection (Liu et al., 2021). LaeNet was tested using Landsat 8 imagery to map the surface area of Selinco Lake (China), employing the Keras framework, Python, and ArcGIS for its implementation. Liu et al. (2024) also achieved real-time mapping of fragmented ponds using an attention-guided U-Net variant – R50A3-LWBENet (Liu et al., 2024b).

3.5.3. Hybrid approaches

In many cases, combining multiple classification methods leads to improved accuracy and robustness in water body mapping. When different approaches, such as machine learning, deep learning, and threshold-based methods, are combined, the strategy is referred to as a hybrid approach (Pimenta et al., 2025). Some studies have integrated unsupervised classification and deep learning techniques, where deep learning serves as a post-processing step to refine the initial results. One such approach, called Unsupervised Curriculum Learning (UCL), was used at a global scale for reservoir surface area determination (Abid et al., 2021). Other research efforts have combined supervised classification, deep learning, and ensemble methods to map water bodies more accurately (He et al., 2017; Tian et al., 2024).

These studies demonstrate that leveraging the strengths of multiple algorithms can significantly enhance mapping outcomes. In a case study focused on delineating small reservoirs from radar imagery in the semi-arid Upper East Region of Ghana, a hybrid method combining unsupervised and supervised classification was employed. Specifically, Maximum Likelihood Classification was applied, with training data provided using ERDAS Imagine (Annor et al., 2009).

3.5.4. Area generation from elevation data

Area generation from elevation data is another approach commonly implemented directly within specialized software tools. It involves using Digital Elevation Models (DEM) to delineate the extent of water bodies based on terrain features. For instance, Khojiakbar et al. (2019) used Global Mapper along with DEM data from the Shuttle Radar Topographic Mission (SRTM) to extract the contours of the Shtepa Reservoir in Uzbekistan (Khasanov et al., 2019). Similarly, this method was applied by Sichangi and Makokha (2017) for the surface area estimation of Lake Victoria, based on the analysis of Landsat imagery combined with elevation information (Sichangi and Makokha, 2017). This technique is particularly useful in areas where elevation differences clearly define the boundaries of water bodies, offering an additional layer of accuracy when optical or radar imagery alone is insufficient.

3.6. Optical sensors for reservoir water level/depth determination

The bathymetry determined by using satellite images is called Satellite-Derived Bathymetry (SDB). The optical satellites used for reservoir surface mapping are often the same ones employed for water level and depth estimation. However, the key distinction lies in the methods of image processing and analysis.

Water level or depth estimation using optical sensors is based on the principles of Electromagnetic Reflectance (EMR) and the Inherent Optical Properties (IOPs) of the water column. As the depth of water increases, the radiant energy of the EMR in the visible wavelengths decreases due to absorption and scattering within the water body (Ashphaq et al., 2021). In practice, water depth is not retrieved directly from EMR or IOPs alone, but through radiative transfer models that use these parameters as inputs to simulate the propagation of light in the water column and infer bottom depth (Gould and Arnone, 1997; Legleiter et al., 2009).

Several factors can limit the accuracy of measurements derived from optical imagery, including atmospheric conditions (e.g., cloud cover, aerosols), composition of the water column (e.g., dissolved organic matter, chlorophyll), presence of suspended sediments, and actual water depth (particularly in cases of high turbidity or very shallow waters) (Ashphaq et al., 2021; Legleiter et al., 2009). The optical sensors commonly utilized by researchers for reservoir water level and depth estimation are summarized in Table 7.

3.7. Altimeters for reservoir water level/depth determination

Satellite altimetry is a remote sensing technique used to measure surface elevation by calculating the time it takes for a signal to travel from the satellite to the Earth's surface and back. Two main types of altimeters are widely employed for water level estimation: radar altimeters and laser altimeters (Gao, 2015).

- **Radar altimeter**

Radar altimeters are active sensors installed on various Earth observation satellites. They operate by emitting radio frequency (RF) pulses – typically in the range of 1.0×10^4 *Hz to* 3.0×10^{11} *Hz* – towards the Earth's surface and recording the time delay of the reflected signal (Birkett, 1994). These sensors can function under all weather conditions and during both day and night, making them ideal for continuous monitoring. Radar altimetry has been extensively used for monitoring inland water levels and reservoir dynamics for several decades (67 % of

Table 7
Some optical sensors for water level/depth estimation.

Sensor group	Documented usage in literature	Satellite	Number of bands	Temporal resolution	Spatial resolution	Coverage area	Availability	Launch date	End date
Medium Spatial Resolution Sensors	6 studies	Landsat 1-9	4 to 9	16 days	30–80 m	Global	Free	1972	–
	1 study	IRS P6 LISS III	4	24 days	23 m	Limited	Free	2003	2013
	4 studies	ASTER	14	16 days	15 m–90 m	Global	Free	1999	–
	6 studies	Sentinel 2	13	5 days	10–60 m	Global	Free	2015	–
High Spatial Resolution Sensors	1 study	GF1	4	4 days	1–16 m	Limited	Commercial	2013	–

the studies). C-band SAR missions remain dominant, yet X-band constellations (e.g., TerraSAR-X/TanDEM-X) and GNSS-R delay–Doppler maps from CYGNSS are increasingly leveraged for sub-kilometer water detection under heavy cloud (Li et al., 2021; Brendle et al., 2024). Reservoir assessments with the SWOT KaRIn interferometer demonstrate centimetric precision (0.10–0.30 m) even along narrow reaches (Zhao et al., 2025). Improved retracking of Sentinel-3A SRAL waveforms successfully help analyze water level over Qinghai Lake, Doroudzan Dam reservoir, and Jiangsu Province lakes and reservoirs (Chen et al., 2025; Xu et al., 2024; Ghanbari et al., 2024). Some commonly used radar altimeters for water level estimation are listed in Table 8.

- **Laser altimeter**

Laser altimeters – commonly referred to as LiDAR (Light Detection and Ranging) – differ from radar altimeters in that they use light pulses instead of radio waves. This gives them significantly higher spatial resolution and accuracy (Falkner et al., 2007). One of the most widely used laser altimeters is the Geoscience Laser Altimeter System (GLAS), mounted on NASA's Ice, Cloud, and Land Elevation Satellite (ICESat). The ICESat/GLAS system operates with a Pulse Repetition Frequency (PRF) of 40 Hz and emits pulses at wavelengths of 1064 nm (infrared) and 532 nm (green). It has a spatial resolution of approximately 60 m × 70 m and a revisit time of 180 days. ICESat was launched in 2003 and remained operational until 2010. Data from GLAS has been widely used in studies of water level variations in lakes and reservoirs (Girard et al., 2025; Zhu et al., 2014; Arsen et al., 2013; Zhang et al., 2014b; Song et al., 2013). ICESat-2 was launched in 2018 (Girard et al., 2025).

3.8. Satellite gravimetry

Satellite gravimetry involves the measurement of variations in the Earth's gravity field over time. This method is particularly useful for monitoring changes in terrestrial water storage, including groundwater, surface water, and soil moisture at large spatial scales. The Gravity Recovery and Climate Experiment (GRACE) mission, launched in 2002, was one of the pioneering satellite missions in this domain. GRACE provided valuable data for water level and mass change estimation and contributed significantly to global hydrological databases such as HYDROWEB, managed by the French Space Agency (Centre National d'Études Spatiales – CNES) (Keys and Scott, 2018). Following the conclusion of the GRACE mission in 2017, the GRACE Follow-On (GFO) mission was launched in 2018 to continue and enhance observations. GRACE and GFO operate with a spatial resolution of approximately 400 km and a temporal resolution of about 30 days, making them suitable for continental and regional-scale hydrological assessments rather than small-scale reservoir monitoring. GRACE/GFO solutions were coupled with Landsat areas to quantify 20-year storage trends in Poyang Lake (Wang et al., 2024).

3.9. Approaches used for reservoir water level/depth determination

In many studies, researchers obtain water level data directly from specialized online platforms and databases (Cheng et al., 2022; Singh et al., 2015; Keys and Scott, 2018; Yuan et al., 2024). These platforms include the Database for Hydrological Time Series of Inland Waters (DAHITI), the Global Reservoir and Lake Monitor (GRLM), the U.S. Department of Agriculture's Global Reservoir and Lake Elevation Database, the French Space Agency's (CNES) HYDROWEB, the European Space Agency's (ESA) River and Lake dataset, and the Global Lakes and Wetlands Database (GLWD). The open-access GloLakes record (1984-present) now provides harmonized altimetry-optical time-series for >27 000 lakes/reservoirs worldwide (Hou et al., 2024). These resources provide valuable, pre-processed water level data derived from satellite observations, facilitating large-scale hydrological analysis.

A key limitation of this approach, however, is the uneven spatial coverage – data availability is often limited in certain regions, particularly in less monitored parts of the Global South. Nonetheless, these platforms offer accessible and reliable datasets for many of the world's large lakes and reservoirs, which can be freely downloaded for research and operational purposes.

3.9.1. Specific approaches for altimeters

Extracting water level data using satellite altimeters is generally straightforward, and in many cases, the specific methods employed are not thoroughly detailed by the authors. For radar altimeters, the water level is typically derived as the difference between the satellite's altitude and the measured distance to the water surface. The basic equation used

Table 8
Some Radar altimeters used for water level estimation.

Satellite	Temporal resolution	Spatial resolution	Coverage area	Availability	Launch date	End date
Sentinel 1	12 days	5 m * 5 m–5 m * 20 m	Global	Commercial	2014	–
TerraSAR-X (TanDEM-X)	3 days	1.1–18.5 m	Global	Commercial	2007	2010
Sentinel 3 SRAL	27 days	300 m * 1.64 Km	Global	Free	2016	–
ENVISAT	35 days	20 Km	Global	Commercial	2002	2012
ERS-1 & 2	2–7 days	50 Km	Global	Commercial	1991	2011
Topex/Poseidon	10 days	11 * 5.1 Km	Global	Free	1992	2005
Jason 1 & 2	10 days	11 * 5.1 Km	Global	Free	2001	2013
SARAL/Altika	35 days	8 Km	Global	Commercial	2013	–
Cosmo SkyMed	16 days	1–100 m	Global	Commercial	2007	–
RADARSAT-2	24 days	3–100 m	Global	Commercial	2002	2012
SRTM	NA	30 m–90 m	Global	Free	2000	–
CYGNSS constellation	1 day	150–250 m	Limited	Free	2016	

for water level estimation is:

$$h = H - R_{obs} - \Delta R$$

where h is the water surface elevation, H is the satellite elevation above a reference ellipsoid provided by a precise orbit solution, R_{obs} is the observed altimeter range, and ΔR includes all range and geophysical corrections (Gao, 2015).

The principle is almost the same for laser altimeters. It is also possible to use the GLAS visualizer and National Snow and Ice Data Center (NSIDC) GLAS Altimetry Elevation Extractor Tool (NGAT) to extract water levels from ICESat images (Song et al., 2013).

3.9.2. Other approaches

Classifying the various approaches used to estimate reservoir water levels can be challenging, as many methods overlap in their principles and applications (Ashphaq et al., 2021). For instance, satellite gravimetry, particularly through Terrestrial Water Storage (TWS) anomalies, provides indirect estimates of water level changes by detecting mass variations in the Earth's gravity field. This type of data is often integrated with other hydrological indicators. More broadly, authors typically employ one or a combination of the following bathymetric estimation methods.

- Empirical SDB approaches

Empirical SDB methods rely on statistically derived relationships between water surface area and corresponding water level or depth, often using linear regression. These relationships assume that a consistent correlation exists between surface area and water level over time. Once a regression equation is established – typically from in situ measurements or elevation data – it can be applied to estimate water levels from satellite-derived surface areas.

A common approach involves using passive (e.g., Landsat, Sentinel-2) and active (e.g., radar altimetry) satellite imagery to determine the reservoir surface area, which is then input into the area – elevation relationship to compute water levels (Codjia et al., 2025; Pipitone et al., 2018; Munyaneza et al., 2009; Vickers et al., 2019; Velpuri et al., 2012). For example, Hossen et al. (2022) developed a linear regression model linking Sentinel-3 Radar Altimeter (SRAL) reflectance with in situ water depth to estimate depth variations in the Aswan High Dam Lake (Hossen et al., 2022).

In addition, elevation data from sources such as TerraSAR-X (TanDEM-X), SRTM, and ASTER can be used to derive water levels. Chipman et al. (2019) applied two different methods: the first estimated water levels by identifying the mean shoreline elevation using fractional surface area (eFrac) maps and a DEM; the second involved computing the cumulative area of DEM pixels below successive elevation increments to match observed surface areas (Chipman, 2019). Similarly, for the Itoiz Reservoir in Spain, Militino et al. (2020) combined Landsat 8, Sentinel-2, and DEM data and used RGISTools to estimate water levels (Militino et al., 2020).

- AI-based SDB

Machine learning approaches have increasingly been employed in SDB to model complex, non-linear relationships between remotely sensed data and water depth or elevation. These methods outperform traditional empirical models in terms of flexibility and accuracy, particularly in heterogeneous environments. Several machine learning algorithms have been explored, including deep learning, supervised classification algorithms, and ensemble classification methods.

In the realm of deep learning, Artificial Neural Networks (ANNs) have been effectively utilized to model complex, non-linear relationships between spectral data and water depth. For instance, Moses et al. (2013) employed ANNs to derive bathymetric information from Indian Remote Sensing (P6-LISS III) satellite imagery, demonstrating the capability of ANNs to handle high-dimensional data patterns (Moses et al., 2013).

Supervised classification algorithms have also been applied to estimate water depths from remote sensing data. Elshazly et al. (2021) explored various algorithms, including Decision Trees, Bagging, Least Squares Boosting (LSB), and Support Vector Machines (SVM), to produce bathymetric maps of Lake Manzala in Egypt using Landsat 8 imagery (Elshazly et al., 2021). Their study highlighted the effectiveness of ensemble methods in handling complex water bodies.

Among ensemble classification methods, Random Forest (RF) classifiers have gained prominence due to their robustness and resistance to overfitting. Sagawa et al. (2019) applied RF algorithms to multi-temporal Landsat data across five different test locations, achieving accurate bathymetric estimations in shallow waters (Sagawa et al., 2019). Similarly, Yunus et al. (2019) demonstrated the effectiveness of RF in various aquatic environments, reinforcing its applicability in SDB (Yunus et al., 2019).

These machine learning approaches are typically implemented using a range of software platforms, including ENVI, ArcGIS, Weka, Google Earth Engine (GEE), SPSS, MATLAB, and ERDAS Imagine, facilitating the processing and analysis of satellite-derived data for bathymetric mapping.

- Physics-based (Analytical) SDB

Physics-based approaches for SDB are grounded in radiative transfer theory, particularly the application of Beer's Law, which models the attenuation of light as it passes through and is scattered and absorbed by the water column. These methods rely on analytical formulations to retrieve bathymetric information, allowing for physically interpretable and often more generalized results. One key application is the derivation of visible bathymetry (VB) – the elevation range between the maximum water extent and the water mask extracted from Digital Elevation Models (DEMs) (Li et al., 2021). Getirana et al. (2018) outlined a systematic four-step methodology to estimate bathymetry based on VB: combining water masks with water level measurements, stacking the water masks by elevation, correcting them to account for errors or inconsistencies, and finally generating bathymetric estimates by linking elevation values to the water mask layers (Getirana et al., 2018).

Additionally, Baup et al. (2014) demonstrated a physics-based method involving the estimation of the height of the reflecting water surface using ENVISAT satellite imagery (Baup et al., 2014). By applying the Virtual Altimetry Station (VALS) technique, they successfully estimated the water level of Lake “La Bure” in southwestern France. Similarly, Casal et al. (2020) employed a model inversion approach using Sentinel-2 data to produce a bathymetric map (Casal et al., 2020). Their method accounted for several inherent water column parameters such as phytoplankton concentration, colored dissolved organic matter (CDOM), particulate backscatter, and depth, thereby enabling a more comprehensive and physically realistic estimation of underwater topography.

- Semi-Empirical SDB

Semi-Empirical SDB approaches are typically applied to optical satellite imagery and represent a hybrid between purely empirical and fully physics-based models. These methods rely on simplified physical assumptions while incorporating empirical calibration to improve performance. Two widely used techniques in this category are the Band Ratio and Band Difference methods, both of which trace their origins to foundational studies by Stumpf et al. (2003) and Lyzenga et al. (2006) (Stumpf et al., 2003; Lyzenga et al., 2006).

The Log-Ratio Model estimates depth (z) using a logarithmic ratio of observed reflectance in different spectral bands. The Linear Band Model represents depth as a linear combination of transformed radiance values across multiple spectral bands. Table 9 presents the formula for these methods.

Several studies have successfully applied these models' using imagery from satellites like Landsat 8, GF-1, and Sentinel-2, processed with tools such as Google Earth Engine (GEE), ENVI, and ArcGIS. For instance, Nan et al. (2020), Traganos et al. (2018), Casal et al. (2019), and El-Sayed (2018) demonstrated the feasibility and accuracy of these semi-empirical approaches for deriving water depth across various aquatic environments (Nan et al., 2020; Casal et al., 2019; El-Sayed, 2018; Traganos et al., 2018).

3.10. Approaches for reservoir volumes estimation

Estimating reservoir volume and its temporal variations is critical for effective water resources management, particularly in data-scarce or transboundary regions. However, satellite sensors cannot directly measure storage volume. Instead, reservoir volume is inferred from remotely sensed parameters such as surface area and water level or depth, often combined with in situ data or digital elevation models (DEMs) (Chawla et al., 2020). Several methods and analytical approaches have emerged to bridge this data gap, depending on the availability of field observations, satellite imagery, and terrain models. Approaches combining optical surface area with altimetry or Digital Elevation Model (DEM) data are the most common methods for determining water volume (approximately 60 %). Water-level–volume regressions are used in about 25 % of cases, while area–volume curves alone account for the remaining 15 %.

- Surface area–based volume estimation

When historical or in situ bathymetric data are available, a mathematical relationship (typically a polynomial or power function) can be established between surface area and volume, known as the Area–Volume (A–V) curve. This curve enables the estimation of reservoir volume on any date for which a satellite-derived surface area measurement exists. Pereira et al. (2019) demonstrated this approach by using Landsat-derived surface areas and fitted A–V relationships for volume prediction (Pereira et al., 2019).

- Water level–based volume estimation

Similarly, when water level measurements and corresponding storage volumes are available, a Height–Volume (H–V) curve can be created. Then, remotely sensed water levels – often derived from satellite altimetry or radar imagery – can be used to estimate storage. This approach is suitable for large reservoirs monitored over time. For example, Baup et al. (2014) used this method to track volume changes in French lakes using ENVISAT altimetry data, while Singh et al. (2015) applied it in India (Baup et al., 2014; Singh et al., 2015). Lu et al. (2013) estimated the volume of Lake Baiyangdian using the Volume Statistics module in ArcMap 9.3's 3D Analyst (Lu et al., 2013). This method requires a DEM of the reservoir bed and a water surface elevation to calculate the volume between the terrain and water surface. On the other hand, Wang et al. (2021) applied non-linear regression models, including the Myquart and Universal Global Optimization (UGO) methods, to improve the accuracy of volume estimations by modeling complex relationships between observed variables and reservoir volume (Wang et al., 2021).

- Volume based on combined water level and surface area

In some cases, only one variable (surface area or water level) is remotely sensed, and the other is missing (Enkhbold et al., 2025). Here, a relationship between the two variables – typically an Area–Height (A–H) curve – can be established. Using this, the missing variable can be inferred, and the existing H–V or A–V curve can be re-expressed in terms of the observed quantity. This chain of transformations allows indirect volume estimation from a single remotely sensed parameter. Arsen et al. (2013) employed this multi-step approach to improve reservoir volume estimates using only surface area data (Arsen et al., 2013).

- Volume variations based on water level and surface area

Storage variation or temporal volume change (ΔV) is another key metric that can be derived from multi-temporal satellite data on Water level and Surface area. Song, Huang, and Ke (2013) proposed a simplified trapezoidal formula to calculate storage variation using sequential measurements of surface area and water level (Song et al., 2013):

$$\Delta V_i = \frac{A_{i-1} + A_i}{2} \times (H_i - H_{i-1})$$

where ΔV_i is the storage variation during a given period; A_{i-1} and A_i refer to the reservoir surface area at times i-1 and i, respectively; H_i and H_{i-1} refer to the water level at times i−1 and i, respectively. This formula assumes a linear change in surface area and water level between time steps $i-1$ and i, allowing the estimation of volume change over the period.

3.11. Performance of estimation

More than 86 % of the papers studied provide at least one quantitative performance metric for their reservoir estimates. Table 10 shows the main accuracy metrics used across the reviewed papers.

Most authors assess the accuracy of reservoir surface area estimation with OA and Kappa (site-specific metrics) derived from confusion matrix and then validate their results using RMSE or PE that compare remotely sensed value to in-situ area records. OA values reach 99 % (Kappa up to 0.9) while RMSE and PE vary greatly depending on the size of the reservoirs. The high spatial resolution of satellites and the use of advanced machine or deep learning approaches contribute to better accuracy. Nurwauziyah et al. (2018) demonstrated that using Pleiades imagery with the Support Vector Machine (SVM) classifier yielded the highest Overall Accuracy (78.6 %), compared to K-Nearest Neighbors (76.26 %) and Decision Tree (68.41 %) (Nurwauziyah et al., 2018). An RMSE of 0.17 km^2 was achieved with multi-spectral 500 m Sentinel-3 SLSTR

Table 9
Some Semi-Empirical SDB models.

Models/ Algorithms	Formula	Reference
Log-Ratio Model	$z = m_1 \frac{ln\left(nR_w(\gamma_i)\right)}{ln\left(nR_w(\gamma_j)\right)} - m_0$ where Z is the depth, n is constant to ensure the ratio remains positive under all values, γi and γj are spectral bands, Rw is the observed reflectance in band, m_0 is the offset, and m_1 is a gain.	Stumpf et al. (2003)
Linear band model	$z = h_0 - \sum_{j=1}^{N} h_j X_j$ where h_0 and each h_j are constants defining a linear relationship between X_j and depth; X_j is transformed radiance for each of the bands 1-N.	Lyzenga et al. (2006)

Table 10
Main accuracy metrics used across the reviewed papers.

Metric	Surface area studies	Water level studies	Volume studies
OA	23	–	–
Kappa	17	–	–
RMSE	104	21	11
R/R^2	16	21	16
MAE	5	–	–
Percent Error	7	–	–

swaths in an arid setting where reservoirs are large and turbidity is low (Hossen et al., 2022). Overall, accuracy is primarily determined by pixel size, cloud/shadow prevalence and aquatic vegetation (as demonstrated by Codjia et al., 2025), as well as the threshold or classifier used (Codjia et al., 2025). While radar mitigates the first two limitations, it can introduce speckles, which degrades the detection of small reservoirs. Multi-sensor fusion consistently outperforms single-sensor mapping of reservoir extent. For instance, Schmitt (2020) study revealed that combining Sentinel-1 and Sentinel-2 data produced an OA of approximately 98.5 % and a Kappa of around 0.97. In contrast, the best single-sensor setup (Sentinel-2 alone) produced lower results, with an OA of about 98.25 % and a Kappa of 0.96 (Schmitt, 2020). The fused image stack reduced false positives and produced more coherent water boundaries. However, limitations remained regarding very small bodies of water due to the 20-m SWIR inputs.

For water-level studies, the preferred statistic is RMSE, which is typically presented alongside R or R^2 to indicate the goodness of fit. Across the case studies, the RMSE varies from a few centimetres to approximately 10 m, depending on the sensor and the retrieval model used. ICESat-2 and Sentinel-3 SRAL are the most accurate (3–10 cm), but this is only true if the waveforms are re-tracked and tied to on-site gauges (e.g. Zhu et al., 2014 (Zhu et al., 2014)). In estimating water level using the Log-transformed Band Ratio Model, Yunus et al. (2019) reported Root Mean Square Errors (RMSEs) ranging from 1.99 to 4.84 m with Sentinel-2 data, and from 2.5 to 5.67 m with Landsat 8 (Yunus et al., 2019). The higher spatial resolution of Sentinel-2 contributed to better accuracy. Accuracy is controlled by the spatial resolution, the vertical precision of the sensor and the retracking algorithm, as well as the temporal mismatch between remote observations and gauge records. The method used also affects accuracy, along with optical interference by clouds, shadows or suspended sediment for passive sensors.

As volume estimation combines the errors of both area and level, authors rely mostly on RMSE and R^2. The most accurate method for deriving volume is based on the use of water level-area (H-A) dataset. Girard et al., 2024 demonstrated that using ICESat-2, Sentinel-3 and synchronous area polygons from Sentinel-2, yielding normalized RMSE between 2.3 and 12.1 % (Girard et al., 2025). When a single area–volume (A–V) regression is fitted to a historic bathymetric survey and the results are compared with those from an optical sensor estimation, RMSE is usually between 3 % and 10 %. Baup et al. (2014) reported an RMSE between 0.2 hm^3 and 0.12 hm^3 for lake “La Bure” (Baup et al., 2014). Therefore, the governing accuracy controls are the temporal density of water level measurements, the spatial resolution and cloud-free availability of shoreline imagery, how fresh and complete the bathymetric data is, and the H–A relationship. Also important is the degree of temporal synchrony between height and area estimation.

3.12. Recommendation on reservoir physical characteristics estimation

The selection of appropriate remote sensing parameters – namely spatial, temporal, and spectral resolutions – must align with the physical characteristics and monitoring objectives of the target reservoir. Spatial resolution should correspond to reservoir size to ensure accurate detection. Temporal resolution influences monitoring frequency, with higher spatial resolution sensors often exhibiting lower revisit rates. For instance, MODIS captures daily imagery at 250–1000 m resolution, while Landsat, with its 30 m spatial resolution, has a 16-day revisit cycle (García et al., 2016).

The choice of sensor type is equally critical. Active sensors, particularly Synthetic Aperture Radar (SAR), offer the advantage of all-weather monitoring by penetrating cloud cover and, in the case of L-band SAR (15–30 cm wavelength), even vegetation canopies (Ottinger and Kuenzer, 2020). However, SAR data often suffer from low spatial and temporal resolution, presence of speckles in the images, and restricted accessibility, limiting their operational use.

Multi-sensor data fusion improves reservoir mapping by combining the strengths of different sensors. For example, SAR can overcome clouds and shadows, while optical sensors provide fine spectral detail. This combination fills gaps and stabilizes surface-area time series across seasons. However, it also introduces practical constraints. Sensors differ in their revisit cycles, spatial resolution, and viewing geometry. Therefore, same-day inputs are often unavailable, making true daily monitoring difficult. Careful harmonization is also required to avoid inconsistencies.

Hybrid approaches, combining spectral water indices and advanced classification methods, are recommended for delineating water surfaces. The integration of water indices with ensemble learning techniques such as Random Forest (RF) has proven robust, including small reservoirs (Codjia et al., 2025; Ghansah et al., 2022). Used alone threshold-based water index methods deliver mean overall accuracies of about 86 % and image-classification approaches including machine learning and deep learning always exceed 90 % accuracy, with CNN reaching 98–99 %.

For small reservoirs, many altimetry and gravity satellites are unsuitable due to their coarse spatial resolution, limiting their ability to capture fine-scale variations. While satellite altimetry can provide reliable water level measurements (Velpuri et al., 2012), the low temporal resolution of both radar and laser altimeters constrains their use for continuous monitoring (Gao, 2015). Optical sensors offer a more practical alternative due to their higher spatial and temporal resolution, but their effectiveness is influenced by factors such as water clarity, depth, and surrounding vegetation (Codjia et al., 2025). In this context, empirical and machine learning models have proven more adaptable than physics-based or semi-empirical approaches, particularly when environmental variability is high. However, aligning in situ water level measurements with satellite acquisition times can pose logistical challenges. A promising solution involves integrating digital elevation model (DEM) data, such as SRTM, with optical imagery from platforms like Sentinel-2 - a method successfully applied by Militino et al. (2020) using R-GIS tools (Militino et al., 2020). Given these insights, the automation of water extent and water level estimation processes is strongly recommended to enable efficient, routine monitoring of small reservoirs.

Accurate volume estimation typically requires in situ validation data, which are often unavailable in ungauged reservoirs. As a result, direct volume estimations from satellite data must be interpreted cautiously. Volume can be estimated using either the surface area–volume curve or the water level–volume curve, depending on which input variable (surface area or water level) has higher accuracy. These methods typically achieve mean errors between 10 % and 20 %. Time-series analysis of volume variation based on these inputs is also recommended.

4. Conclusion

Reservoirs are strategic infrastructures for water storage, supply regulation, irrigation, and climate resilience – particularly in regions facing increasing water stress due to climate variability. The review of satellite-based approaches to estimating reservoir surface area, water level, and volume reveals significant progress in remote sensing technologies, yet also underscores critical methodological, technical, and contextual limitations that must be addressed to enhance their operational utility.

The evolution of satellite missions – ranging from optical to radar and altimetry sensors—has enabled more frequent and spatially detailed observations of water bodies. However, limitations persist with respect to sensor trade-offs (e.g., spatial vs. temporal resolution), data accessibility, and the adaptability of certain techniques across diverse geographic and ecological settings. While SAR and altimetry provide significant advantages under cloud or canopy cover, their coarse spatial resolution or restricted coverage hampers their standalone application in small or fragmented reservoirs. Similarly, optical sensors, although widely available and detailed, can be affected by atmospheric interference, turbidity, and seasonal vegetation growth around reservoirs.

Among the methods reviewed, hybrid techniques combining spectral indices, machine learning, DEM integration, and ensemble classification emerge as the most robust for surface area extraction and water level estimation. Nevertheless, accurate volume estimation continues to depend on auxiliary data such as bathymetric surveys or in situ validation, which are often unavailable or outdated, particularly in remote or ungauged basins.

The study also highlights the lack of standardized workflows or universally accepted accuracy metrics for evaluating remote sensing-based reservoir estimations. While a variety of accuracy indicators – such as Precision, Recall, POD, Kappa coefficient, mIoU, and others – have been employed across studies, their inconsistent application limits comparability and validation. Furthermore, automated monitoring systems, although technically feasible, remain underutilized in practice due to computational, infrastructural, or capacity constraints in many low-resource settings.

In view of these gaps, future research should prioritize the development of integrated, open-access platforms that combine multi-source satellite data, in situ observations, and AI for near-real-time reservoir monitoring. Efforts should also focus on customizing methodologies to local contexts, especially for small and seasonal reservoirs that dominate semi-arid and tropical regions. Long-term validation studies using harmonized accuracy metrics across diverse biophysical and climatic zones are essential to ensure comparability and robustness of results. Interdisciplinary collaborations between hydrologists, remote sensing scientists, data engineers, and local water managers to co-design operational tools and data pipelines, will be required to advance this field. Finally, sustained policy and institutional support is crucial to ensure that remote sensing products are effectively translated into actionable water governance strategies and planning frameworks.

Ultimately, advancing the reliability and applicability of satellite remote sensing for reservoir physical characteristics estimation offers a transformative opportunity. It can strengthen early warning systems, inform climate-smart agriculture, and support equitable water allocation – contributing meaningfully to resilience-building and sustainable development in vulnerable regions.

CRediT authorship contribution statement

Audrey Kantz Dossou Codjia: Writing – original draft, Visualization, Methodology, Formal analysis, Data curation, Conceptualization. **Komlavi Akpoti:** Writing – review & editing, Resources, Methodology, Conceptualization. **Moctar Dembélé:** Writing – review & editing, Resources, Methodology, Conceptualization. **Roland Yonaba:** Writing – review & editing, Supervision, Methodology. **Tazen Fowe:** Writing – review & editing, Supervision, Conceptualization. **Triumph Prosper Orowale:** Writing – review & editing, Formal analysis, Data curation. **Modeste G. Déo-Gratias Koissi:** Validation, Methodology, Conceptualization. **Soumahila Sankande:** Resources, Methodology, Conceptualization. **Sander J. Zwart:** Writing – review & editing, Supervision, Methodology, Funding acquisition, Conceptualization.

Declaration of generative AI and AI-assisted technologies in the writing process

During the preparation of this work, the authors used ChatGPT to improve language and readability. After using this tool, the authors reviewed and edited the content as needed and took full responsibility for the content of the publication.

Declaration of competing interest

The authors declare that they have no known competing financial interests or personal relationships that could have appeared to influence the work reported in this paper.

Acknowledgments

This study was conducted as part of the DIWASA (Digital Innovations for Water Secure Africa) project of the International Water Management Institute (IWMI). The authors gratefully acknowledge The Leona M. and Harry B. Helmsley Charitable Trust for their financial support. The authors express their gratitude to IWMI and 2iE (International Institute for Water and Environmental Engineering) for overseeing the entire research process.

Data availability

The References section lists all of the research articles that were used to produce the review.

References

Abd R., Ellah, El-Geziry, T., 2016. Bathymetric study of some khors in Lake Nasser, Egypt. Lake. Reserv. Pond. 10 (2), 139–158.
Abid, N., Shahzad, M., Malik, M.I., et al., 2021. UCL: unsupervised curriculum learning for water body classification from remote sensing imagery. Int. J. Appl. Earth Obs. Geoinf. 105, 102568.
Akpoti, K., Kabo-bah, A.T., Zwart, S.J., 2019. Agricultural land suitability analysis: State-of-the-art and outlooks for integration of climate change analysis. Agric. Syst. 173, 172–208.
Akpoti, K., Higginbottom, T.P., Foster, T., Adhikari, R., Zwart, S.J., 2022. Mapping land suitability for informal, small-scale irrigation development using spatial modelling and machine learning in the upper East Region, Ghana. Sci. Total Environ. 803, 149959.
Amitrano, D., Di Martino, G., Iodice, A., et al., 2017. Mapping small reservoirs in semi-arid regions using multitemporal SAR: methods and applications. In: 2017 9th International Workshop on the Analysis of Multitemporal Remote Sensing Images (MultiTemp). IEEE, pp. 1–4.
Annor, F.O., Van de Giesen, N., Liebe, J., Van de Zaag, P., Tilmant, A., Odai, S.N., 2009. Delineation of small reservoirs using radar imagery in a semi-arid environment: a case study in the upper east region of Ghana. Phys. Chem. Earth, Parts A/B/C 34 (4–5), 309–315.
Arsen, A., Crétaux, J.F., Berge-Nguyen, M., Abarca del Rio, R., 2013. Remote sensing-derived bathymetry of Lake Poopó. Remote Sens (Basel). 6 (1), 407–420.
Ashphaq, M., Srivastava, P.K., Mitra, D., 2021. Review of near-shore satellite derived bathymetry: classification and account of five decades of coastal bathymetry research. J. Ocean Eng. Sci. 6 (4), 340–359.
Ashraf, A., Ahmad, L., Ferooz, K., et al., 2023. Remote sensing as a management and monitoring tool for agriculture: potential applications. Int. J. Environ. Clim. Chang. 13, 324–343.
Baup, F., Frappart, F., Maubant, J., 2014. Combining high-resolution satellite images and altimetry to estimate the volume of small lakes. Hydrol. Earth Syst. Sci. 18 (5), 2007–2020.
Bijeesh, T.V., Narasimhamurthy, K.N., 2020. Surface water detection and delineation using remote sensing images: a review of methods and algorithms. Sustain. Water Resour. Manag. 6 (4), 68.
Birkett, C.M., 1994. Radar altimetry: a new concept in monitoring lake level changes. Eos, Trans. Amer. Geophys. Union 75 (24), 273–275.
Birkett, C.M., 2000. Synergistic remote sensing of Lake Chad: variability of basin inundation. Remote Sens. Environ. 72 (2), 218–236.
Brendle, N.J., Chan, S.K., Hajj, G., Al-Khaldi, M.M., Johnson, J.T., 2024. Reservoir water level monitoring using CYGNSS's Level-1 observations. IEEE J. Sel. Top. Appl. Earth Obs. Rem. Sens. 17, 9090–9098. https://doi.org/10.1109/JSTARS.2024.3384111.
Brisco, B., 2015. Mapping and monitoring surface water and wetlands with synthetic aperture radar. Rem. Sens. Wetlands: Appl. Adv. 119–136. Published online.
Cao, H., Zhang, H., Wang, C., Zhang, B., 2019. Operational flood detection using Sentinel-1 SAR data over large areas. Water (Basel) 11 (4), 786.
Carbonneau, P.E., 2025. Style transfer from Sentinel-1 to Sentinel-2 for fluvial scenes with multi-modal and multi-temporal image fusion. Remote Sens (Basel) 17 (20), 3445. https://doi.org/10.3390/rs17203445.
Casal, G., Monteys, X., Hedley, J., Harris, P., Cahalane, C., McCarthy, T., 2019. Assessment of empirical algorithms for bathymetry extraction using Sentinel-2 data. Int. J. Rem. Sens. 40 (8), 2855–2879.
Casal, G., Hedley, J.D., Monteys, X., Harris, P., Cahalane, C., McCarthy, T., 2020. Satellite-derived bathymetry in optically complex waters using a model inversion approach and Sentinel-2 data. Estuar. Coast Shelf Sci. 241, 106814.
Ceylan, A., Karabork, H., Ekozoglu, I., 2011. An analysis of bathymetric changes in Altinapa reservoir. Carpath. J. Earth Environ. Sci. 6 (2), 15–24.
Chawla, I., Karthikeyan, L., Mishra, A.K., 2020. A review of remote sensing applications for water security: quantity, quality, and extremes. J. Hydrol. (Amst.) 585, 124826.
Chen, J., Wang, Y., Wang, J., et al., 2024. The performance of Landsat-8 and Landsat-9 data for water body extraction based on various water indices: a comparative analysis. Remote Sens (Basel). 16 (11), 1984.
Chen, C., Li, X., Zhu, J., et al., 2025. Research on the Algorithm of Lake Surface height inversion in Qinghai Lake based on Sentinel-3A altimeter. Remote Sens (Basel). 17 (4), 647.

Cheng, J., Song, C., Liu, K., et al., 2022. Satellite and UAV-based remote sensing for assessing the flooding risk from Tibetan lake expansion and optimizing the village relocation site. Sci. Total Environ. 802, 149928.
Chi, M., Plaza, A., Benediktsson, J.A., Sun, Z., Shen, J., Zhu, Y., 2016. Big data for remote sensing: challenges and opportunities. Proc. IEEE 104 (11), 2207–2219.
Chipman, J.W., 2019. A multisensor approach to satellite monitoring of trends in lake area, water level, and volume. Remote Sens (Basel). 11 (2), 158.
Codjia, A.K.D., Akpoti, K., Dembélé, M., et al., 2025. Estimating water levels in reservoirs using Sentinel-2 derived time series of surface water areas: a case study of 20 reservoirs in Burkina Faso. Int. J. Appl. Earth Obs. Geoinf. 139, 104523.
Congalton, R.G., 2001. Accuracy assessment and validation of remotely sensed and other spatial information. Int. J. Wildland Fire 10 (4), 321–328.
Crétaux, J.F., Biancamaria, S., Arsen, A., Bergé-Nguyen, M., Becker, M., 2015. Global surveys of reservoirs and lakes from satellites and regional application to the Syrdarya river basin. Environ. Res. Lett. 10 (1), 015002.
Crist, E.P., 1985. A TM tasseled cap equivalent transformation for reflectance factor data. Remote Sens. Environ. 17 (3), 301–306.
Dardanelli, G., La, Loggia G., Perfetti, N., Capodici, F., Puccio, L., Maltese, A., 2014. Monitoring displacements of an earthen dam using GNSS and remote sensing. Rem. Sens. Agricult. Ecosyst. Hydrol. XVI 9239, 923928. https://doi.org/10.1117/12.2071222. SPIE.
Declaro, A., Kanae, S., 2024. Enhancing surface water monitoring through multi-satellite data-fusion of Landsat-8/9, Sentinel-2, and Sentinel-1 SAR. Remote Sens (Basel). 16 (17). https://doi.org/10.3390/rs16173329.
Donchyts, G., Winsemius, H., Baart, F., et al., 2022. High-resolution surface water dynamics in Earth's small and medium-sized reservoirs. Sci. Rep. 12 (1), 13776. https://doi.org/10.1038/s41598-022-17074-6.
Druce, D., Tong, X., Lei, X., et al., 2021. An optical and SAR based fusion approach for mapping surface water dynamics over mainland China. Remote Sens (Basel) 13 (9). https://doi.org/10.3390/rs13091663.
Duy, N.B., 2015. Automatic detection of surface water bodies from Sentinel-1 SAR images using valley-Emphasis method. Vietnam J. Earth Sci. 37 (4), 328–343.
El-Sayed, M.S., 2018. Comparative study of satellite images performance in mapping lake bathymetry: case study of Al-Manzala Lake, Egypt. Am. J. Geogr. Inf. Syst. 7 (3), 82–87.
Eldardiry, H., Hossain, F., 2021. The value of long-term streamflow forecasts in adaptive reservoir operation: the case of the High Aswan dam in the transboundary nile river basin. J. Hydrometeorol. 22 (5), 1099–1115.
Elshazly, R.E., Armanuos, A.M., Zeidan, B.A., Elshemy, M., 2021. Evaluating remote sensing approaches for mapping the bathymetry of Lake manzala, Egypt. EuroMediterr. J. Environ. Integr. 6 (3). https://doi.org/10.1007/s41207-021-00285-0.
Enkhbold, A., Vandansambuu, B., Yadamsuren, G., et al., 2025. Estimation of morphometric parameters of lakes based on satellite imagery data: implications of relationships between lakes in the arid region of western Mongolia, Central Asia. Quaest. Geogr. 44 (1), 21–38.
Falkner, P., Peacock, A., Schulz, R., 2007. Instrumentation for planetary exploration missions. Planets and Moons 10, 595–641.
Famiglietti, J.S., 2014. The global groundwater crisis. Nat. Clim. Change 4 (11), 945–948. https://doi.org/10.1038/nclimate2425. Nature Publishing Group.
Feyisa, G.L., Meilby, H., Fensholt, R., Proud, S.R., 2014. Automated water extraction index: a new technique for surface water mapping using landsat imagery. Remote Sens. Environ. 140, 23–35. https://doi.org/10.1016/j.rse.2013.08.029.
Filali, Boubrahimi S., Neema, A., Nassar, A., Hosseinzadeh, P., Hamdi, S.M., 2024. Spatiotemporal data augmentation of MODIS-landsat water bodies using adversarial networks. Water Resour. Res. 60 (3). https://doi.org/10.1029/2023WR036342.
Fisher, A., Flood, N., Danaher, T., 2016. Comparing landsat water index methods for automated water classification in eastern Australia. Remote Sens. Environ. 175, 167–182. https://doi.org/10.1016/j.rse.2015.12.055.
Gan, M., Feng, L., Shao, J., et al., 2025. Satellite observations reveal declining diatom concentrations in the three gorges reservoir: the impacts of dam construction and local climate. Remote Sens (Basel). 17 (2). https://doi.org/10.3390/rs17020309.
Gao, H., 2015. Satellite remote sensing of large lakes and reservoirs: from elevation and area to storage. WIREs Water 2 (2), 147–157. https://doi.org/10.1002/wat2.1065.
Gao, H., Birkett, C., Lettenmaier, D.P., 2012a. Global monitoring of large reservoir storage from satellite remote sensing. Water Resour. Res. 48 (9). https://doi.org/10.1029/2012WR012063.
Gao, H., Birkett, C., Lettenmaier, D.P., 2012b. Global monitoring of large reservoir storage from satellite remote sensing. Water Resour. Res. 48 (9). https://doi.org/10.1029/2012WR012063.
García, L., Rodríguez, J., Wijnen, M., Pakulski, I., 2016. Earth Observation for Water Resources Management: Current Use and Future Opportunities for the Water Sector. https://doi.org/10.1596/978-1-4648-0475-5.
Garnier, J., Cicerelli, R.E., de Almeida, T., et al., 2024. Water resources monitoring in a remote region: earth observation-based study of endorheic Lakes. Remote Sens (Basel). 16 (15). https://doi.org/10.3390/rs16152790.
Getirana, A., Jung, H.C., Tseng, K.H., 2018. Deriving three dimensional reservoir bathymetry from multi-satellite datasets. Remote Sens. Environ. 217, 366–374. https://doi.org/10.1016/j.rse.2018.08.030.
Ghanbari, R., Tayfehrostami, A., Forouzanfar, M., Tashakori, M., 2024. Using optical satellite images and satellite altimetry data to estimate volume variations in dams. Int. Arch. Photogramm. Rem. Sens. Spatial Inform. Sci. - ISPRS Arch. 48, 189–196. https://doi.org/10.5194/isprs-archives-XLVIII-4-W9-2024-189-2024. International Society for Photogrammetry and Remote Sensing.
Ghansah, B., Foster, T., Higginbottom, T.P., Adhikari, R., Zwart, S.J., 2022. Monitoring spatial-temporal variations of surface areas of small reservoirs in Ghana's upper east region using Sentinel-2 satellite imagery and machine learning. Phys. Chem. Earth, Parts A/B/C 125, 103082. https://doi.org/10.1016/j.pce.2021.103082.
Ghebreyesus, D.T., Temimi, M., Fares, A., Bayabil, H.K., 2016. Remote sensing applications for monitoring water resources in the UAE using Lake Zakher as a water storage gauge. In: Fares, A. (Ed.), Emerging Issues in Groundwater Resources. Springer International Publishing, pp. 145–157. https://doi.org/10.1007/978-3-319-32008-3_6.
Girard, F., Kergoat, L., Nikiema, H., et al., 2025. Comparison of methods to derive the height-area relationship of shallow Lakes in West Africa using remote sensing. Water Resour. Res. 61 (2). https://doi.org/10.1029/2024WR037411 e2024WR037411.
Goetz, A.F.H., Rock, B.N., Rowan, L.C., 1983. Remote sensing for exploration; an overview. Econ. Geol. 78 (4), 573–590. https://doi.org/10.2113/gsecongeo.78.4.573.
Gould, R.W., Arnone, R.A., 1997. Remote sensing estimates of inherent optical properties in a coastal environment. Remote Sens. Environ. 61 (2), 290–301. https://doi.org/10.1016/S0034-4257(97)89496-5.
Grimaldi, S., Li, Y., Pauwels, V.R.N., Walker, J.P., 2016. Remote sensing-derived water extent and level to constrain hydraulic flood forecasting models: opportunities and challenges. Surv. Geophys. 37 (5), 977–1034. https://doi.org/10.1007/s10712-016-9378-y.
Guerschman, J., Warren, G., Byrne, G., Lymburner, L., Mueller, N., van Dijk, A., 2011. MODIS-based Standing Water Detection for Flood and Large Reservoir Mapping: Algorithm Development and Applications for the Australian Continent.
Hahmann, T., Wessel, B., 2010. Surface water body detection in high-resolution TerraSAR-X data using active contour models. In: 8th European Conference on Synthetic Aperture Radar, pp. 1–4.
He, A., He, J., Kim, R., Like, D., Yan, A., 2017. An ensemble-based approach for classification of high-resolution satellite imagery of the amazon basin. In: 2017 IEEE MIT Undergraduate Research Technology Conference (URTC), pp. 1–4. https://doi.org/10.1109/URTC.2017.8284189.
Hossain, A.K.M.A., Mathias, C., Blanton, R., 2021. Remote sensing of turbidity in the tennessee river using landsat 8 satellite. Remote Sens (Basel) 13 (18). https://doi.org/10.3390/rs13183785.
Hossen, H., Khairy, M., Ghaly, S., Scozzari, A., Negm, A., Elsahabi, M., 2022. Bathymetric and capacity relationships based on Sentinel-3 mission data for Aswan high dam Lake, Egypt. Water (Basel). 14 (5). https://doi.org/10.3390/w14050711.
Hostache, R., Matgen, P., Wagner, W., 2012. Change detection approaches for flood extent mapping: how to select the most adequate reference image from online archives? Int. J. Appl. Earth Obs. Geoinf. 19, 205–213. https://doi.org/10.1016/j.jag.2012.05.003.
Hou, J., Van Dijk, A.I.J.M., Renzullo, L.J., Larraondo, P.R., 2024. GloLakes: water storage dynamics for 27000 lakes globally from 1984 to present derived from satellite altimetry and optical imaging. Earth Syst. Sci. Data 16 (1), 201–218. https://doi.org/10.5194/essd-16-201-2024.
Huang, C., Chen, Y., Zhang, S., Wu, J., 2018. Detecting, extracting, and monitoring surface water from space using optical sensors: a review. Rev. Geophys. 56 (2), 333–360. https://doi.org/10.1029/2018RG000598.
Jiang, H., Feng, M., Zhu, Y., Lu, N., Huang, J., Xiao, T., 2014. An automated method for extracting rivers and lakes from landsat imagery. Remote Sens (Basel). 6 (6), 5067–5089. https://doi.org/10.3390/rs6065067.
Jiang, D., Li, Y., Liu, Q., Huang, C., 2024. Evaluating the sustainable development science satellite 1 (SDGSAT-1) multi-spectral data for river water mapping: a comparative study with Sentinel-2. Remote Sens (Basel). 16 (15). https://doi.org/10.3390/rs16152716.
Kale, S., Acarlı, D., 2019. Spatial and temporal change monitoring in water surface area of atikhisar reservoir (Çanakkale, Turkey) by using remote sensing and geographic information system techniques. Alinteri J. Agricult. Sci. 34 (1), 47–56. https://doi.org/10.28955/alinterizbd.574361.
Keys, T.A., Scott, D.T., 2018. Monitoring volumetric fluctuations in tropical lakes and reservoirs using satellite remote sensing. Lake Reserv. Manag. 34 (2), 154–166. https://doi.org/10.1080/10402381.2017.1402226.
Khan, S.I., Hong, Y., Wang, J., et al., 2011. Satellite remote sensing and hydrologic modeling for flood inundation mapping in Lake Victoria basin: implications for hydrologic prediction in ungauged basins. IEEE Trans. Geosci. Rem. Sens. 49 (1), 85–95. https://doi.org/10.1109/TGRS.2010.2057513.
Khasanov, K., Masharif, B., Jamshid, C., Aziz, J., Azat, K., 2019. Water reservoir area and volume determination using geoinformation technologies and remote sensing. Chem. Eng. Technol. 8, 2277–3878. https://doi.org/10.35940/ijrte.D8089.118419.
Kislik, C., Dronova, I., Grantham, T.E., Kelly, M., 2022. Mapping algal bloom dynamics in small reservoirs using Sentinel-2 imagery in Google Earth Engine. Ecol. Indic. 140, 109041. https://doi.org/10.1016/j.ecolind.2022.109041.
Kong, Y., Jimenez, K., Lee, C.M., et al., 2025. Monitoring coastal water turbidity using Sentinel2—A case Study in Los Angeles. Remote Sens (Basel). 17 (2). https://doi.org/10.3390/rs17020201.
Krivoguz, D., Mal'ko, S., Borovskaya, R., Semenova, A., 2020. Automatic processing of Sentinel-2 image for Kerch peninsula lake areas extraction using QGIS and python. E3S Web Conf. 203. https://doi.org/10.1051/e3sconf/202020303011.
Leblanc, M., Lemoalle, J., Bader, J.C., Tweed, S., Mofor, L., 2011. Thermal remote sensing of water under flooded vegetation: new observations of inundation patterns for the "Small" Lake Chad. J. Hydrol. (Amst.) 404 (1–2), 87–98. https://doi.org/10.1016/j.jhydrol.2011.04.023.
Legleiter, C., Roberts, D., Lawrence, R., 2009. Spectrally based remote sensing of river bathymetry. Earth Surf. Process. Landf. 34, 1039–1059. https://doi.org/10.1002/esp.1787.
Li, Y., Gao, H., Allen, G.H., Zhang, Z., 2021. Constructing reservoir area–volume–elevation curve from TanDEM-X DEM data. IEEE J. Sel. Top. Appl.

Earth Obs. Rem. Sens. 14, 2249–2257. https://doi.org/10.1109/JSTARS.2021.3051103.
Li, M., Hong, L., Guo, J., Zhu, A., 2022. Automated extraction of lake water bodies in complex geographical environments by fusing sentinel-1/2 data. Water (Switzerland) 14 (1). https://doi.org/10.3390/w14010030.
Li, Y., Zhao, G., Allen, G.H., Gao, H., 2023. Diminishing storage returns of reservoir construction. Nat. Commun. 14 (1), 3203. https://doi.org/10.1038/s41467-023-38843-5.
Li, Y., Li, S., Cheng, L., Zhou, L., Chang, L., Liu, P., 2024. High spatiotemporal estimation of Reservoir evaporation water loss by integrating remote-sensing data and the generalized complementary relationship. Remote Sens (Basel). 16 (8). https://doi.org/10.3390/rs16081320.
Liu, W., Chen, X., Ran, J., et al., 2021. LaeNet: a novel lightweight multitask CNN for automatically extracting Lake area and shoreline from remote sensing images. Remote Sens (Basel). 13 (1). https://doi.org/10.3390/rs13010056.
Liu, Y., Wang, C., Jiang, C., et al., 2024a. Water storage capacity estimation for a large complex lake system incorporating the water levels during flooding season. J Hydrol Reg Stud. 51, 101634. https://doi.org/10.1016/j.ejrh.2023.101634.
Liu, M., Liu, J., Hu, H., 2024b. A novel deep learning network model for extracting Lake water bodies from remote sensing images. Appl. Sci. 14 (4). https://doi.org/10.3390/app14041344.
Lu, S., Wu, B., Yan, N., Wang, H., 2011. Water body mapping method with HJ-1A/B satellite imagery. Int. J. Appl. Earth Obs. Geoinf. 13 (3), 428–434. https://doi.org/10.1016/j.jag.2010.09.006.
Lu, S., Ninglei, O., Bingfang, W., Yongping, W., Tesemma, Z., 2013. Lake water volume calculation with time series remote-sensing images. Int. J. Rem. Sens. 34 (22), 7962–7973. https://doi.org/10.1080/01431161.2013.827814.
Lyzenga, D.R., Malinas, N.P., Tanis, F.J., 2006. Multispectral bathymetry using a simple physically based algorithm. IEEE Trans. Geosci. Rem. Sens. 44 (8), 2251–2259. https://doi.org/10.1109/TGRS.2006.872909.
Ma, X., Wang, L., Chen, C., Du, J., Sun, S., 2020. Simulation of the dynamic water storage and its gravitational effect in the head region of three gorges reservoir using imageries of gaofen-1. Remote Sens (Basel). 12 (20), 1–20. https://doi.org/10.3390/rs12203353.
Ma, Q., Gui, X., Duan, Z., Li, J., Li, Y., Xiong, L., 2024. Daily Reservoir Inflow and Water Storage Estimation Through Integration of Multi-Source Satellite Imagery and Hydrological Modeling in Data-Scarce Basins. https://doi.org/10.2139/ssrn.4995728.
McFEETERS, S.K., 1996. The use of the normalized difference water index (NDWI) in the delineation of open water features. Int. J. Rem. Sens. 17 (7), 1425–1432. https://doi.org/10.1080/01431169608948714.
Militino, A.F., Montesino-SanMartin, M., Pérez-Goya, U., Ugarte, M.D., 2020. Using RGISTools to estimate water levels in reservoirs and lakes. Remote Sens (Basel) 12 (12). https://doi.org/10.3390/rs12121934.
Minghelli, A., Spagnoli, J., Lei, M., Chami, M., Charmasson, S., 2020. Shoreline extraction from worldview2 satellite data in the presence of foam pixels using multispectral classification method. Remote Sens (Basel) 12 (16). https://doi.org/10.3390/RS12162664.
Miura, Y., Shamsudduha, M., Suppasri, A., Sano, D., 2025. A global multi-sensor dataset of surface water indices from Landsat-8 and Sentinel-2 satellite measurements. Sci. Data 12 (1). https://doi.org/10.1038/s41597-025-05562-z.
Mohebzadeh, H., Fallah, M., 2019. Quantitative analysis of water balance components in Lake Urmia, Iran using remote sensing technology. Remote Sens. Appl. 13, 389–400. https://doi.org/10.1016/j.rsase.2018.12.009.
Moses, S.A., Janaki, L., Joseph, S., Gomathi, J.P., Joseph, J., 2013. Lake bathymetry from Indian remote sensing (P6-LISS III) satellite imagery using artificial neural network model. Lakes Reserv. 18 (2), 145–153. https://doi.org/10.1111/lre.12027.
Munyaneza, O., Wali, U.G., Uhlenbrook, S., Maskey, S., Mlotha, M.J., 2009. Water level monitoring using radar remote sensing data: application to Lake Kivu, central Africa. Phys. Chem. Earth, Parts A/B/C 34 (13), 722–728. https://doi.org/10.1016/j.pce.2009.06.008.
Mylona, E., Daskalopoulou, V., Sykioti, O., Koutroumbas, K., Rontogiannis, A., 2018. Classification of Sentinel-2 images utilizing abundance representation. Proc. West Mark. Ed. Assoc. Conf. 2 (7). https://doi.org/10.3390/ecrs-2-05141.
Nan, Y., Jianhui, L., Wenbo, M., et al., 2020. Water depth retrieval models of East Dongting Lake, China, using GF-1 multi-spectral remote sensing images. Glob. Ecol. Conserv. 22, e01004. https://doi.org/10.1016/j.gecco.2020.e01004.
Niño, F., Coggiola, C., Blumstein, D., Lasson, L., Calmant, S., 2022. Monitoring of inland water levels by satellite altimetry and deep learning. IEEE Trans. Geosci. Rem. Sens. 60, 1–14. https://doi.org/10.1109/TGRS.2021.3138329.
Noruzi, A., 2005. Google scholar: the new generation of citation indexes, 55 (4), 170–180. https://doi.org/10.1515/LIBR.2005.170.
Nurwauziyah, I., Sulistyah, U., Gede, I., Putra, I.G.B., Firdaus, M., 2018. Satellite Image Classification Using Decision Tree. SVM and k-Nearest Neighbor. Published online July 11.
Ottinger, M., Kuenzer, C., 2020. Spaceborne L-Band synthetic aperture radar data for geoscientific analyses in coastal land applications: a review. Remote Sens (Basel). 12 (14). https://doi.org/10.3390/rs12142228.
Ouma, Y.O., Tateishi, R., 2006. A water index for rapid mapping of shoreline changes of five East African rift valley lakes: an empirical analysis using Landsat TM and ETM+ data. Int. J. Rem. Sens. 27 (15), 3153–3181. https://doi.org/10.1080/01431160500309934.
Pang, Z., Jin, Q., Fan, P., et al., 2023. Deformation monitoring and analysis of reservoir Dams based on SBAS-InSAR technology—banqiao Reservoir. Remote Sens (Basel) 15 (12). https://doi.org/10.3390/rs15123062.
Peng, C., Liu, Y., Chen, L., et al., 2025. An accuracy assessment of the ESTARFM data-fusion model in monitoring Lake dynamics. Water (Switzerland) 17 (14). https://doi.org/10.3390/w17142057.
Pereira, B., Pedro, M., Till, F., Geraldo, R., Saskia, F., De Araújo, J.C., 2019. Assessment of the geometry and volumes of small surface water reservoirs by remote sensing in a semi-arid region with high reservoir density. Hydrol. Sci. J. 64 (1), 66–79. https://doi.org/10.1080/02626667.2019.1566727.
Pham-Duc, B., Prigent, C., Aires, F., 2017. Surface water monitoring within Cambodia and the Vietnamese mekong Delta over a year, with Sentinel-1 SAR observations. Water (Switzerland) 9 (6). https://doi.org/10.3390/w9060366.
Pimenta, J., Fernandes, J.N., Azevedo, A., 2025. Remote sensing tool for reservoir volume estimation. Remote Sens (Basel). 17 (4). https://doi.org/10.3390/rs17040619.
Pipitone, C., Maltese, A., Dardanelli, G., Lo Brutto, M., La Loggia, G., 2018. Monitoring water surface and level of a reservoir using different remote sensing approaches and comparison with dam displacements evaluated via GNSS. Remote Sens (Basel). 10 (1). https://doi.org/10.3390/rs10010071.
Psomiadis, E., Tomanis, L., Kavvadias, A., Soulis, K.X., Charizopoulos, N., Michas, S., 2021. Potential dam breach analysis and flood wave risk assessment using HEC-RAS and remote sensing data: a multicriteria approach. Water (Basel) 13 (3). https://doi.org/10.3390/w13030364.
Quang, D.N., Linh, N.K., Tam, H.S., Viet, N.T., 2021. Remote sensing applications for reservoir water level monitoring, sustainable water surface management, and environmental risks in Quang Nam province, Vietnam. J. Water Clim. Change 12 (7), 3045–3063. https://doi.org/10.2166/wcc.2021.347.
Rao, P., Lou, L., Jiang, W., Cao, X., Wang, Y., Wang, X., 2019. Continuous dynamics monitoring of multi-lake water extent using a spatial and temporal adaptive fusion method based on two sets of MODIS products. Sensors (Switzerland) 19 (22). https://doi.org/10.3390/s19224873.
Rey, D.M., Walvoord, M., Minsley, B., Rover, J., Singha, K., 2019. Investigating lake-area dynamics across a permafrost-thaw spectrum using airborne electromagnetic surveys and remote sensing time-series data in Yukon flats, Alaska. Environ. Res. Lett. 14 (2), 025001. https://doi.org/10.1088/1748-9326/aaf06f.
Rodríguez-Alarcón, R., Lozano, S., 2017. SOM-based decision support system for reservoir operation management. J. Hydrol. Eng. 22 (7), 04017012. https://doi.org/10.1061/(ASCE)HE.1943-5584.0001496.
Sagawa, T., Yamashita, Y., Okumura, T., Yamanokuchi, T., 2019. Satellite derived bathymetry using machine learning and multi-temporal satellite images. Remote Sens (Basel) 11 (10). https://doi.org/10.3390/rs11101155.
Sarp, G., Ozcelik, M., 2017. Water body extraction and change detection using time series: a case study of Lake Burdur, Turkey. J. Taibah Univ. Sci. 11 (3), 381–391. https://doi.org/10.1016/j.jtusci.2016.04.005.
Schmitt, M., 2020. Potential of large-scale inland water body mapping from Sentinel-1/2 data on the example of bavaria's Lakes and Rivers. PFG - J. Photogramm. Rem. Sens. Geoinform. Sci. 88 (3–4), 271–289. https://doi.org/10.1007/s41064-020-00111-2.
Şen, Z., 2021. Reservoirs for water supply under climate change impact—A review. Water Resour. Manag. 35 (11), 3827–3843. https://doi.org/10.1007/s11269-021-02925-0.
Sethre, P.R., Bradley, C.R., Todhunter, P.E., 2005. Remote detection of prairie pothole ponds in the devils Lake basin, North Dakota. GIsci. Rem. Sens. 42 (4), 277–296. https://doi.org/10.2747/1548-1603.42.4.277.
Sheffield, J., Wood, E.F., Pan, M., et al., 2018. Satellite remote sensing for water resources management: potential for supporting sustainable development in data-poor regions. Water Resour. Res. 54 (12), 9724–9758. https://doi.org/10.1029/2017WR022437.
Shen, X., Anagnostou, E.N., Allen, G.H., Robert Brakenridge, G., Kettner, A.J., 2019. Near-real-time non-obstructed flood inundation mapping using synthetic aperture radar. Remote Sens. Environ. 221, 302–315. https://doi.org/10.1016/j.rse.2018.11.008.
Sichangi, A.W., Makokha, G.O., 2017. Monitoring water depth, surface area and volume changes in Lake Victoria: integrating the bathymetry map and remote sensing data during 1993–2016. Model Earth Syst. Environ. 3 (2), 533–538. https://doi.org/10.1007/s40808-017-0311-2.
Singh, A., Kumar, U., Seitz, F., 2015. Remote sensing of storage fluctuations of poorly gauged reservoirs and state space model (SSM)-based estimation. Remote Sens (Basel). 7 (12), 17113–17134. https://doi.org/10.3390/rs71215872.
Soltani, K., Amiri, A., Zeynoddin, M., Ebtehaj, I., Gharabaghi, B., Bonakdari, H., 2021. Forecasting monthly fluctuations of lake surface areas using remote sensing techniques and novel machine learning methods. Theor. Appl. Climatol. 143 (1), 713–735. https://doi.org/10.1007/s00704-020-03419-6.
Song, C., Huang, B., Ke, L., 2013. Modeling and analysis of lake water storage changes on the Tibetan Plateau using multi-mission satellite data. Remote Sens. Environ. 135, 25–35. https://doi.org/10.1016/j.rse.2013.03.013.
Sorkhabi, O.M., Shadmanfar, B., Kiani, E., 2022. Monitoring of dam reservoir storage with multiple satellite sensors and artificial intelligence. Results Eng. 16, 100542. https://doi.org/10.1016/j.rineng.2022.100542.
Stumpf, R.P., Holderied, K., Sinclair, M., 2003. Determination of water depth with high-resolution satellite imagery over variable bottom types. Limnol. Oceanogr. 48 (1part2), 547–556. https://doi.org/10.4319/lo.2003.48.1_part_2.0547.
Tavus, B., Kocaman, S., Nefeslioglu, H.A., Gokceoglu, C., 2020. A fusion approach for flood mapping using sentinel-1 and sentinel-2 datasets. Int. Arch. Photogramm. Rem. Sens. Spatial Inform. Sci. - ISPRS Arch. 43, 641–648. https://doi.org/10.5194/isprs-archives-XLIII-B3-2020-641-2020. International Society for Photogrammetry and Remote Sensing.

Tian, H., Li, W., Wu, M., et al., 2017. Dynamic monitoring of the largest freshwater Lake in China using a new water index derived from high spatiotemporal resolution Sentinel-1A data. Remote Sens (Basel). 9 (6). https://doi.org/10.3390/rs9060521.
Tian, D., Zhao, X., Gao, L., et al., 2024. Estimation of water quality variables based on machine learning model and cluster analysis-based empirical model using multi-source remote sensing data in inland reservoirs, South China. Environ. Pollut. 342, 123104. https://doi.org/10.1016/j.envpol.2023.123104.
Traganos, D., Poursanidis, D., Aggarwal, B., Chrysoulakis, N., Reinartz, P., 2018. Estimating satellite-derived bathymetry (SDB) with the google earth engine and sentinel-2. Remote Sens (Basel) 10 (6), 859.
Vanthof, V., Kelly, R., 2019. Water storage estimation in ungauged small reservoirs with the TanDEM-X DEM and multi-source satellite observations. Remote Sens. Environ. 235, 111437. https://doi.org/10.1016/j.rse.2019.111437.
Velpuri, N.M., Senay, G.B., Asante, K.O., 2012. A multi-source satellite data approach for modelling Lake Turkana water level: calibration and validation using satellite altimetry data. Hydrol. Earth Syst. Sci. 16 (1), 1–18. https://doi.org/10.5194/hess-16-1-2012.
Vickers, H., Malnes, E., Høgda, K.A., 2019. Long-term water surface area monitoring and derived water level using synthetic aperture radar (SAR) at Altevatn, a medium-sized arctic lake. Remote Sens (Basel). 11 (23). https://doi.org/10.3390/rs11232780.
Wada, Y., Bierkens, M.F.P., de Roo, A., et al., 2017. Human–water interface in hydrological modelling: current status and future directions. Hydrol. Earth Syst. Sci. 21 (8), 4169–4193. https://doi.org/10.5194/hess-21-4169-2017.
Wang, J., Yang, S., Liu, H., Wang, P., Lou, H., Gong, T., 2021. Simulation of lake water volume in ungauged terminal lake basin based on multi-source remote sensing. Remote Sens (Basel). 13 (4), 1–20. https://doi.org/10.3390/rs13040697.
Wang, Y., Long, D., Li, X., 2023a. High-temporal-resolution monitoring of reservoir water storage of the lancang-mekong river. Remote Sens. Environ. 292, 113575. https://doi.org/10.1016/j.rse.2023.113575.
Wang, Z., Liu, X., Li, W., He, S., Zheng, T., 2023b. Temporal and spatial variation analysis of Lake area based on the ESTARFM model: a case study of qilu Lake in Yunnan province, China. Water (Switzerland) 15 (10). https://doi.org/10.3390/w15101800.
Wang, F., Zhou, Q., Gao, H., Wen, Y., Zhou, S., 2024. Dynamic monitoring of Poyang Lake water area and storage changes from 2002 to 2022 via remote sensing and satellite gravimetry techniques. Remote Sens (Basel) 16 (13), 2408.
Weng, Z., Li, Q., Zheng, Z., Wang, L., 2025. SCR-Net: a dual-channel water body extraction model based on multi-spectral remote sensing imagery—A case study of Daihai Lake, China. Sensors 25 (3). https://doi.org/10.3390/s25030763.
Wu, G., Liu, Y., 2015. Capturing variations in inundation with satellite remote sensing in a morphologically complex, large lake. J. Hydrol. (Amst.) 523, 14–23. https://doi.org/10.1016/j.jhydrol.2015.01.048.
Wu, G., Chen, C., Liu, Y., Fan, X., Niu, H., Liu, Y., 2023. Developing a high-resolution seamless surface water extent time-series over Lake Victoria by integrating MODIS and landsat data. Remote Sens (Basel) 15 (14). https://doi.org/10.3390/rs15143500.
Xu, H., 2006. Modification of normalised difference water index (NDWI) to enhance open water features in remotely sensed imagery. Int. J. Rem. Sens. 27 (14), 3025–3033. https://doi.org/10.1080/01431160600589179.
Xu, J., Xia, M., Ferreira, V.G., Wang, D., Liu, C., 2024. Estimating and assessing monthly water level changes of reservoirs and Lakes in Jiangsu Province using Sentinel-3 radar altimetry data. Remote Sens (Basel). 16 (5). https://doi.org/10.3390/rs16050808.
Yılmaz, İ., Selim, S., 2024. Comparison of Machine Learning-based and Spectral Index-Supported Image Classification Algorithms Using the Google Earth Engine (GEE) Platform, pp. 39–58.
Yuan, C., Zhang, F., Liu, C., 2024. A comparison of multiple DEMs and satellite Altimetric data in lake volume monitoring. Remote Sens (Basel). 16 (6), 974.
Yunus, A.P., Dou, J., Song, X., Avtar, R., 2019. Improved bathymetric mapping of coastal and lake environments using sentinel-2 and landsat-8 images. Sensors (Switzerland) 19 (12). https://doi.org/10.3390/s19122788.
Zhang, S., Gao, H., Naz, B.S., 2014a. Monitoring reservoir storage in South Asia from multisatellite remote sensing. Water Resour. Res. 50 (11), 8927–8943. https://doi.org/10.1002/2014WR015829.
Zhang, S., Gao, H., Naz, B.S., 2014b. Monitoring reservoir storage in South Asia from multisatellite remote sensing. Water Resour. Res. 50 (11), 8927–8943. https://doi.org/10.1002/2014WR015829.
Zhang, G., Chen, W., Li, G., Yang, W., Yi, S., Luo, W., 2020. Lake water and glacier mass gains in the northwestern Tibetan Plateau observed from multi-sensor remote sensing data: implication of an enhanced hydrological cycle. Remote Sens. Environ. 237, 111554. https://doi.org/10.1016/j.rse.2019.111554.
Zhao, Y., Fu, J., Pang, Z., Jiang, W., Zhang, P., Qi, Z., 2025. Validation of inland water surface elevation from SWOT satellite products: a case study in the middle and lower reaches of the yangtze river. Remote Sens (Basel) 17 (8). https://doi.org/10.3390/rs17081330.
Zheng, D., Lv, A., 2025. MosaicFormer: a novel approach to remote sensing spatiotemporal data fusion for Lake water monitors. Remote Sens (Basel). 17 (7). https://doi.org/10.3390/rs17071138.
Zhu, W., Jia, S., Lv, A., 2014. Monitoring the fluctuation of Lake Qinghai using multi-source remote sensing data. Remote Sens (Basel). 6 (11), 10457–10482. https://doi.org/10.3390/rs61110457.
Zhu, L., Juha, S., Liu, J., Hyyppä, J., Kaartinen, H., Haggren, H., 2017. A review: remote sensing sensors. In: Rustamov, R.B., Hasanova, S., Zeynalova, M.H. (Eds.), Multi-Purposeful Application of Geospatial Data. IntechOpen. https://doi.org/10.5772/intechopen.71049.
Zou, Z., Dong, J., Menarguez, M.A., et al., 2017. Continued decrease of open surface water body area in Oklahoma during 1984–2015. Sci. Total Environ. 595, 451–460. https://doi.org/10.1016/j.scitotenv.2017.03.259.